5-2018

Trim24 in Normal & Malignant Hematopoiesis

Justin Shaw

TRIM24 IN NORMAL AND MALIGNANT HEMATOPOIESIS

A

THESIS

Presented to the Faculty of

The University of Texas

MD Anderson Cancer Center UTHealth

Graduate School of Biomedical Sciences

in Partial Fulfillment

of the Requirements

for the Degree of

MASTER OF SCIENCE

by

Justin Parker Shaw, B.S.
Houston, Texas

May, 2018

Acknowledgments:

I would like to sincerely thank all of my committee members: Dr. Michelle Barton, Dr. Xiaobing Shi, Dr. Zeev Estrov, and Dr. George Eisenhoffer. All of their efforts and insight have been invaluable to the development of my project.

I would also like to give a special thanks to my lab manager, Sabrina Stratton. She has gone above and beyond the call of duty for a lab manager, and has been instrumental to the continued work involved with my project, as well as my professional development.

I would also like to thank my lab members: Dr. Kylee Veazey, Dr. Prosun Das, and Hieu Van. Each of them have not only provided assistance with experiments, but also emotional support and friendship throughout the entirety of my project.

Moreover, I would like to give a sincere thanks to all of the staff of GSBS for the hard work they do to ensure the students have an appropriate learning environment. Each member of GSBS staff I have encountered have gone the extra mile to ensure I have the best experience possible at GSBS.

I would like to give the greatest thanks of all to my dear parents, Charla and Richard Shaw. You have always been there for me. I couldn't thank you enough for always believing in me, and for going so far in preparing me for my future. I love both of you so much.

TRIM24 in Normal and Malignant Hematopoiesis

Justin Parker Shaw, B.S.

Advisory Professor: Margarida Santos, Ph.D.

Treatment for acute myeloid leukemia (AML) has changed little in the past four decades. For the majority of AML patients, current treatment options include chemotherapy and allogeneic stem cell transplants, which also involves high-dose chemotherapy or radiation treatment. These options have little success in the long-run, as only an estimated 26% of patients survive five years post-diagnosis. In efforts to address this low survival rate, interest has increased for targeting epigenetic pathways in AML. This focus stems from the discovery that AML is frequently driven by blockades on hematopoietic stem cell differentiation, which involves a series of coordinated epigenetic changes. Given its reported roles as an epigenetic reader, stem cell regulator, and known oncogene, we investigated *TRIM24* for putative relevance in AML. Expression data from previous studies have also suggested roles for *TRIM24* in chronic myeloid leukemia and acute lymphocytic leukemia; however, no studies to date have reported measurements of *TRIM24* in AML from an *in vivo* system. Here, we report that low *TRIM24* mRNA expression in human AML patients (in TCGA) correlates with poor survival. Additionally, this association was found to be independent of gene expression signatures of prognostic significance, such as Gentles leukemic stem cell signature. Furthermore, loss of *Trim24* in murine, *MLL-AF9*-driven AML worsened survival and increased leukemic stem cell numbers, while having no observed effects on normal hematopoiesis. These results lay the groundwork for future investigations of the role of *TRIM24* in AML, which has the potential to aid development of novel therapeutic strategies.

Table of Contents:

List of Figures:

List of Tables:

Introduction & Background:

Hematopoiesis – an overview:

Hematopoiesis is the process through which all blood cells are produced. In humans and other mammals, this process takes place primarily within the bone marrow beginning as early as embryonic day 15 in mice (1), and month 4 in humans (2). The hematopoietic system's primary responsibilities are conferring immunity and implementing transportation within an organism, being the primary entity responsible for the transportation of nutrients, oxygen, hormones, waste products, and immune cells. The broad range of functions required of this system are carried out by an array of highly specialized hematopoietic cell types, each differing vastly in morphology and function. Moreover, the constant use of these cell populations leads to a high turnover rate of hematopoietic cells, and thus bestows an immense demand for cell production on the hematopoietic system, producing roughly 10^{11} hematopoietic cells daily (3). To cope with both the demands for cell variety and number, the functionally-disparate cell types which comprise the hematopoietic system are all produced from a single hierarchy of differentiation & self-

Figure 1: Overview of the hematopoietic hierarchy

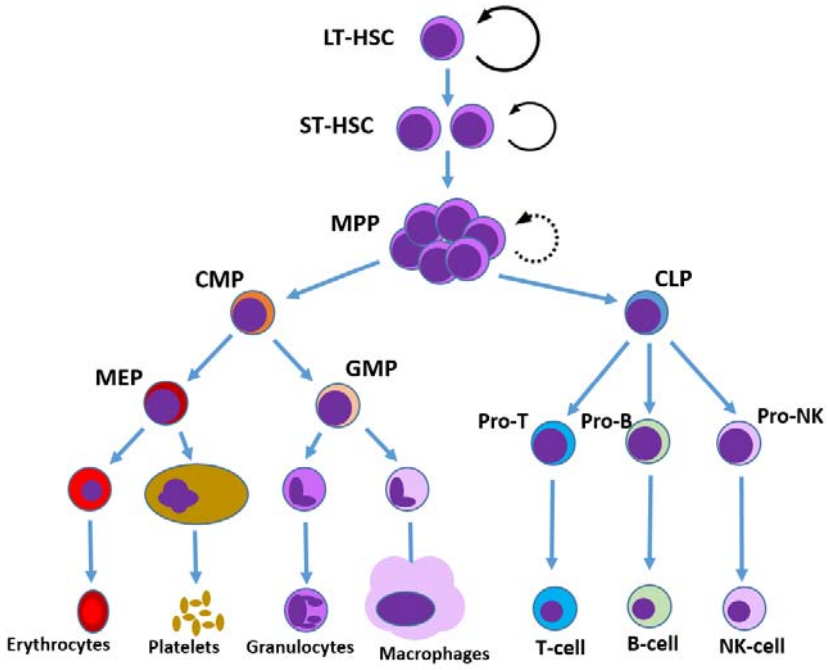

renewal (i.e. differentiation cascade), originating from a small group of stem and progenitor cells in the bone marrow.

This hierarchy is headed by hematopoietic stem cells (HSCs), morphologically indistinct, immature quiescent cells which have the greatest capacity for self-renewal and the slowest rate of division within the hierarchy. HSCs comprise approximately 1 in 10^8 nucleated marrow cells (non-red blood cells) in human bone marrow (3), dividing once approximately every 40 weeks (4). Categorically, these HSCs are further sub-divided into long-term (LT) and short term (ST) HSCs, with ST-HSCs displaying increased rates of division, and LT-HSCs possessing heightened quiescence and self-renewal capability (5, 6). This dichotomy among HSCs adds an additional layer to the hierarchy, thus further diluting the burden of replicative stress on the bone marrow. These HSCs can divide both symmetrically or asymmetrically to yield multipotent progenitor cells (MPPs) (5, 6). MPPs have a lower capacity for self-renewal compared to HSCs, but, conversely, have a higher rate of division (5-7). As the name implies, MPPs are capable of further differentiating into multiple more specialized progenitor cells, and are more directly responsible for meeting the cellular demands imposed on the bone marrow. MPPs differentiate into one of many lineage-committed progenitors, which subsequently divide and differentiate into the mature effector cells of the hematopoietic system, such as erythrocytes, platelets, granulocytes, macrophages, T-cells, B-cells, and NK cells. Granulocytes and macrophages are derived from common myeloid progenitors (CMPs), erythrocytes and platelets are derived from megakaryocyte-erythrocyte progenitors (MEPs) (which themselves can be derived from CMPs or MPPs), and T-cells, natural killer cells, and B-cells are derived from common lymphoid progenitors (CLPs). This extensive hierarchy of self-renewal and differentiation provides an elegant system in which all the hematopoietic cell types required by an organism can be produced while minimizing divisions within the HSC pool. While recent evidence suggests this hierarchical

system may not be as rigid as previously thought (8-10), this model effectively captures the general strategy through which a single human HSC division can lead to the production of over 1 x 10^7 hematopoietic cells (4, 11).

The HSC is the centerpiece of the hematopoietic system, being crucial for maintaining the fidelity of all hematopoiesis. As such, the self-renewal, proliferation, and differentiation of HSCs are each governed by a multitude of epigenetic and extracellular mechanisms, all of which coordinate together as part of the hematopoietic stem cell niche. More specifically, the HSC niche is the culmination of physical and biochemical cues from surrounding adipocytes, nerve cells, osteoclasts, osteoblasts, endothelial cells, mesenchymal cells, blood vessels, and sinusoids in the bone marrow. This specialized microenvironment enforces tight regulations on all HSC activities, and is partly responsible for preventing malignant expansion of the stem cell pool (12, 13).

Hematopoietic malignancy:

The hematopoietic system is inherently prone to malignancies, as the demand for cell production on the hematopoietic system is high in comparison to other tissues (14-17). The hematopoietic system has evolved specific mechanisms to counter this replicative stress, the most notable of which are the aforementioned hierarchy and niche. Additional mechanisms, such as regulation by P53 and common apoptotic pathways, help to further counteract effects of the immense replicative stress intrinsic to the bone marrow (18-20). In spite of these mechanisms, an estimated 173,000 hematopoietic cancers were diagnosed in 2017 within the United States, in addition to 10,000 – 20,000 neoplasms and proliferative disorders such as myelodysplastic syndrome (MDS) (21). Roughly one-third of these cases were leukemia, with 60,000 new cases of leukemia diagnosed in the United States each year and a corresponding 24,000 deaths, accounting for roughly 4% of all new cancer cases and deaths (21). Roughly 380,000 people are

living with leukemia at any time in the US, with an average 5-year survival rate just over 60% (21).

Depending on the maturation level of malignant cells, leukemias are generally classified as chronic or acute, with acute leukemia having a more severe blockade on cell differentiation, and thus a more profound impediment on hematopoietic cell function and patient survival time (21). Both chronic and acute leukemias are further categorized by the cell types the malignancies most closely resemble, and are thought to partly reflect the cell type from which the malignancy originated (22-24). The most common types are lymphocytic and myeloid, but mixed lineage leukemias are also observed (25-28). Among these, Acute Myeloid Leukemia (AML) patients have an unfavorable prognosis, with a 5-year survival rate of only 26% (21). These also constitute roughly a third of all leukemia patients, with approximately 21,000 new cases and 10,500 fatalities annually (21). Acute Myeloid Leukemia (AML), as the name indicates, is an acute leukemia in which cells display a myeloid phenotype. AML is also frequently described as a malignancy of the HSC niche, being that this hematological malignancy originates almost exclusively from hematopoietic stem and progenitor cells (HSPCs) within the bone marrow (29-31). Malignant transformation of HSPCs gives rise to leukemic initiating cells (LICs), a completely self-renewing population of leukemic cells largely agreed to be responsible for driving progression of the disease (29-31). AML can be further sub-divided by utilizing the French-American-British (FAB) classification system for AML, which classifies AML cases based on the cell type the malignant cells most closely resemble (26). In this system, the subtypes M0 – M7 correspond with levels of cellular maturation, with M0 patients displaying the least differentiated cells, and M4-M7 patients displaying more mature cell types (26). This classification system is still broadly used, but in recent years has been more frequently used in conjunction with molecular markers, such as point mutations and chromosomal abnormalities (32).

While 5-year survival for all leukemias has nearly quadrupled since 1960, AML 5-year survival rates hover at approximately 26%, as most drugs have proven to be ineffective in the long-term (21, 33, 34). The exception is all-trans retinoic acid (ATRA), approved by the FDA in 1995 to treat the M3 FAB subtype of AML (34-36). This subtype of AML, also known as acute promyeloitic leukemia (APL), frequently harbors a translocation which results in the expression of a *PML-RARα* fusion protein, halting differentiation in the promyeloitic stage. The APL treatment ATRA operates on a concept known as differentiation therapy, which works by forcing the self-renewing, immature populations of malignancies to terminally differentiate, hence ablating their ability to sustain long-term proliferation and disease. Specifically for APL, this terminal-differentiation is induced by disrupting signaling from the *PML-RARα* fusion protein, thus removing the underlying cause for the differentiation blockade (36). While the role of ATRA is currently limited to the M3 subtype of AML, this treatment is an exemplar for demonstrating the feasibility of differentiation therapies, potentially serving as an archetype for future treatments. As such, exploiting differentiation pathways among hematopoietic cells or targeting pathways necessary for maintaining pluripotency have become key areas of interest for leukemia research.

Epigenetics in Acute Myeloid Leukemia:

In accordance with its relevance for the future of differentiation therapy, epigenetics plays a central role for the development of acute myeloid leukemia. This is largely evident from patient sequencing data obtained within the past decade, revealing that over 40% of patients do not have an identifiable mutation in a signaling gene (such as *KRAS* or *NRAS*), and that over 70% of patients have at least one non-synonymous mutation in an epigenetic modifier (37). Moreover, these mutations have been frequently identified in genes with global epigenetic influence on the genome, such as *DNMT3A* and *TET2* (37). This information, together with gene expression and

amplification data obtained from childhood and adult AML cases, has demonstrated that aberrant epigenetic signatures are a universal theme in human leukemia (37, 38). This prevalence supports the notion that epigenetic dysregulation is paramount for the initiation or maintenance of hematopoietic malignancies. The pervasive involvement of epigenetics in AML is perhaps best understood when interpreted in the context of what is currently known about normal hematopoiesis. The transition from HSC to mature effector cell is a series of coordinated epigenetic changes. As such, any alteration in an epigenetic pathway could lead to a failed step in the differentiation hierarchy. Any such block on differentiation has the potential to result in the eventual development of a hematopoietic malignancy, such as AML. These observations and rationale have recently demonstrated utilitarian value in the clinic, as methylation profiling has been used to classify subtypes of AML with prognostic significance (39-42). Similarly, methylation profiling has been used to predict the stemness of patients' AML, with stemness itself being negatively associated with survival, and highly informative about a patient's progression and response to treatment (43, 44). However, this significance appears to not solely be limited to epigenetic modifiers. An increasing amount of evidence suggests that epigenetic readers, proteins which interact with epigenetic modifications to enact changes in gene expression or chromatin organization, also play a role in leukemic progression (45, 46). This knowledge extends putative relevance in AML to any gene participating in epigenetic pathways, be it through enzymatic or merely associative means.

Fusion genes in Acute Myeloid Leukemia:

The importance of epigenetics in leukemia was first recognized through the study of chromosomal abnormalities in patients, as clinical observations revealed that recurring translocations in leukemia patients produced fusion proteins frequently involving at least one epigenetic modifier, such as *MLL*, *MOZ*, *CBP*, *P300*, or *NSD1* (37). Such chromosomal

translocations are common in AML, being present in 30% of non-complex karyotype patients (47). Prognoses vary substantially across patients with each fusion-protein, with patients harboring *MLL*-fusion proteins among the poorest (48-50). In genetically normal cells, the *MLL* gene (KMT2A) produces an H3K4 methyltransferase tasked with maintaining appropriate expression of the HOXA cluster, a collection of genes which positively regulates self-renewal and stemness in hematopoietic stem and progenitor cells (HSPCs). Upon forming a fusion protein, the *MLL* complex co-localizes (by virtue of its nature) with its fusion partner to *MLL*-target locations within the genome, thereby also recruiting complexes the fusion partner may associate with. *MLL*-fusion leukemia is further subdivided by translocation partner, with over 80 fusion partners being described in the literature (51). The most common fusion partners for *MLL* in AML are *AF9*, *ENL*, *AF10*, *ELL*, and *AF4* (51), all of which are members of the super elongation complex (SEC), a large multi-protein complex responsible for exerting global effects on transcription (51-54). In AML, *MLL*-fusion proteins alter both the recruitment and activity of SEC and DOT1L (H3K79 methyltransferase) to enforce aberrantly high HOXA cluster expression (52, 55). Consequently, this powerful combination of epigenetic modifications and global changes in the transcriptional program in *MLL*-fusion AML patients leads to a blockade on differentiation and malignant transformation of HSPCs.

Akin to results from ATRA treatment in M3 AML, recent evidence suggests differentiation blockades in *MLL*-fusion leukemia can be circumnavigated (56); however, unlike the direct targeting of the *PML-RARa* fusion in M3 AML, differentiation therapy in *MLL*-fusion AML will likely be enacted through targeting other epigenetic pathways. For example, epigenetic modifiers previously unappreciated in AML, such as protein-arginine methyltransferase 5 (PRMT5), have been demonstrated to be therapeutically relevant targets for removing the differentiation blockade and reducing self-renewal capacity in both mouse models and human cell

lines (57). Such discoveries highlight the importance for searching for proteins with epigenetic writing or reading ability, and experimentally assaying their potential relevance for *MLL*-fusion AML treatments and differentiation therapies.

TRIM24 as an Epigenetic Reader and a Regulator of P53:

TRIM24 is a member of the Tripartite Motif-containing (TRIM) family, a superfamily known for E3 ubiquitin ligase activity as well as regulation of autophagy and innate immunity (58, 59). *TRIM24* is located on the distal end of the q-arm of chromosome 7 in humans, and produces a 1050 amino acid, 117 kDA protein (60). TRIM24 possesses an RBBCC domain towards the N-terminus, consisting of of a RING domain, a B-box, and a coiled-coil. This domain is followed by an LXXLL motif (NR box) starting at amino acid 754, and a PHD and Bromo domain at the C-terminus (58-63). The RING domain of TRIM24 confers the enzymatic function of an E3 ubiquitin ligase, and has been demonstrated to directly target p53 for proteasomal degradation (61, 62). Furthermore, TRIM24 has also been shown to participate in a negative regulatory feedback-loop with p53 in a manner similar to that of MDM2 (61). Meanwhile, the PHD domain of TRIM24 has been shown to preferentially bind Histone 3 Lysine 4 in the unmethylated state (H3K4me0), while the Bromo domain of TRIM24 has been demonstrated to preferentially associate with Histone 3 Lysine 23 in the acetylated state (H3K23ac)(63). Via histone peptide arrays, the simultaneous binding of both histone marks has been demonstrated to be critical for the independent association (i.e. in the absence of other proteins) of TRIM24 with chromatin (63). This association has been demonstrated to only be favorable in the cis-conformation, as other arrangements have poor binding kinetics (63). The simultaneous presence of both of these chromatin marks represents a non-canonical histone signature, the roles of which have yet to be fully investigated (63).

Originally known as Transcription Intermediary Factor 1 Alpha (*Tif1α*), the first study on *Trim24* was published in 1995, which reported *Trim24* as a component of the mouse hepatocellular carcinoma fusion oncoprotein, T18 (64, 65). At the time of this study, *TRIM24*'s known roles were limited to interactions with nuclear receptors and enhancement of retinoic acid receptor signaling (65). While informative, *TRIM24* research remained little beyond the scope of nuclear receptor signaling until the Barton lab demonstrated its role as a p53-targeting E3 ubiquitin ligase in 2009 (66). Knowledge of *TRIM24* has since expanded drastically, with demonstrated roles in Wnt, PI3K/Akt, and STAT signaling, as well as in innate immunity, pluripotency, and embryonic stem cell transcription (67-74). Through manipulating these pathways, overexpression of *TRIM24* has been demonstrated to influence a wide variety of human malignancies, including breast cancer, head & neck cancer, glioblastoma, non-small-cell lung cancer, prostate cancer, cervical cancer, and hepatocellular carcinoma (63, 70, 75-81). In the case of hepatocellular carcinoma, both overexpression and deletion of *TRIM24* lead to malignancy (78, 79). This indicates that the role for *TRIM24* may not be as simple as that of a typical oncogene, but may rather be part of a balancing act in preventing oncogenesis, requiring regulation in a precise, context-dependent manner. This balancing act may hold relevance for so far uninvestigated malignancies with respect to *TRIM24*, the prospect of which warrants further investigation.

Rationale – *TRIM24*'s Putative Role in AML:

The functional abilities of TRIM24, and the pathways they regulate, make the gene an interesting candidate for examining its therapeutic relevance in AML. Accordingly, *TRIM24* has recently been within the focus of gene expression studies conducted on both ALL and CML samples (82, 83). In CML, *TRIM24* expression was elevated in the late stages of CML, suggesting it may play a role in the transition to blast crisis, the most advanced form of the disease (83).

Conversely, in ALL, *TRIM24* mRNA expression was associated with favorable patient status, as patients expressing higher levels of *TRIM24* mRNA displayed a lower percentage of blast cells (undifferentiated cells) 28 days post-diagnosis (82). In both cases, the data suggests that *TRIM24* may affect pathways central to the malignant hematopoietic state. As is the case with hepatocellular carcinoma, the above data suggests that *TRIM24* may play a balancing act in leukemia, potentially exhibiting varied, context-dependent effects on hematopoietic malignancies. If and how this may relate to Trim24 in AML has yet to be determined. As acute leukemias generally share more similarities than they do with chronic leukemias, *TRIM24* is more likely to affect AML in a manner similar to how it affects ALL, than CML. To this end, a review of the literature revealed that the genomic location of *TRIM24* (chromosome 7q) is deleted in roughly 10% of both AML and MDS patients, and is associated with a poor prognosis in both instances (84, 85). An additional search among data available in The Cancer Genome Atlas (TCGA) AML dataset revealed that patients above mean *TRIM24* mRNA expression survived roughly 1.8 times longer than patients below mean *TRIM24* mRNA expression (p-value 0.0003) (figure 2).

Figure 2: *TRIM24* mRNA correlates with human survival

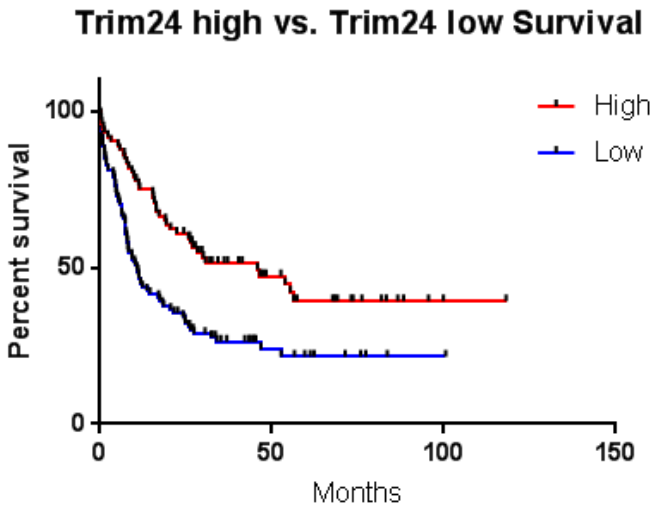

Y-axis represents percent of surviving patients while x-axis represents months of patient survival post-diagnosis. *TRIM24* high expressing patients (red) and *TRIM24* low expressing patients (blue) were separated into their respective groups based on their *TRIM24* expression in comparison to the mean *TRIM24* expression of the group. All data in this figure was obtained from TCGA.

These combined data have led us to **hypothesize that loss of *TRIM24* promotes the progression & aggressiveness of AML**. Moreover, AML is characterized by the aberrant

expression of genes crucial for hematopoietic development & maintenance. This, coupled with the demonstrated roles for *TRIM24* in regulating embryonic stem cell expression & pluripotency, has led us to also **hypothesize that *TRIM24* plays an important role in normal hematopoiesis**. To address these hypotheses, we aim to characterize the role of *TRIM24* in acute myeloid leukemia, and define its role in normal hematopoiesis (detailed in figure 3).

Figure 3: Aims of study

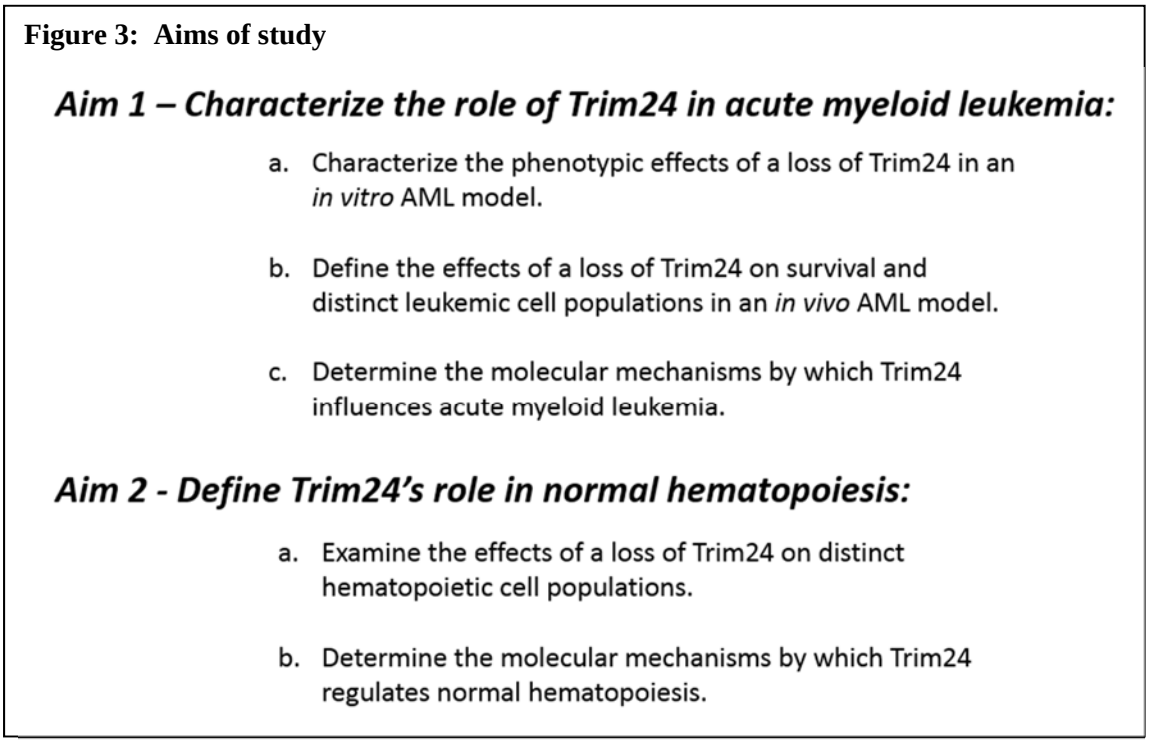

Results:

Colony formation:

In order to gauge the self-renewal capacity of *MLL-AF9* transformed leukemic bone marrow for both *Trim24* wildtype and *Trim24* knockout cells, colony formation assays were performed in a semisolid medium supplemented with cytokines. For passage 1, the colony formation assays (n=3) yielded an average of 151.7 ± 42.4 colonies for *Trim24* knockout cells and 60.7 ± 20.2 colonies for wildtype cells. The difference between these two groups is 91 colonies, with a p-value of 0.12. For passage 2, the *Trim24* knockouts averaged 166.7 ± 46.8 colonies, and the wildtypes averaged 66.7 ± 22.1 colonies, with a difference of 100 between the two groups and a p-value of 0.13. For passage 3, the *Trim24* knockouts averaged 183.3 ± 63.5 colonies, and the wildtypes averaged 68.6 ± 36.7 colonies, with a 114.7 difference between the two groups, and a p-value of 0.19.

Figure 4: *Trim24* knockout cells have increased colony formation ability

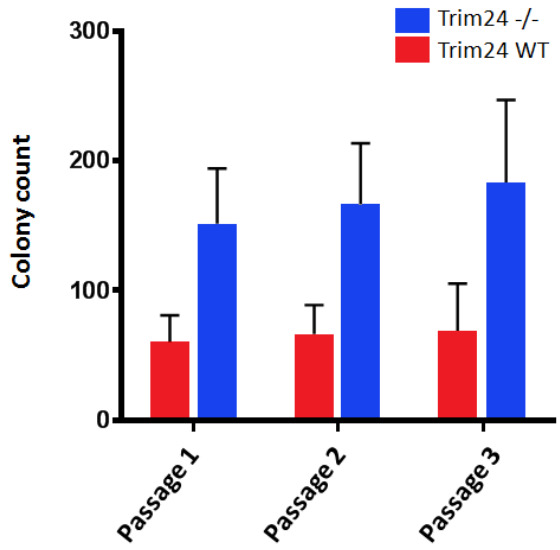

The y-axis represents total colony count per passage, while the x-axis contains the categories for *Trim24* wildtype (red), and *Trim24* knockout (blue), for each passage of cells in the experiment (3 in total).

Cell counts:

In order to gauge for potential effects on proliferation, cell counts were performed on several passages of *Trim24* wildtype and *Trim24* knockout cells in semisolid media (n=3). *Trim24* wildtype cells produced an average of 2.5 ± 0.5 x 10^6 cells per passage, whereas *Trim24* knockout cells produced an average of 3.56 ± 0.1 x 10^6 cells per passage. This yields a roughly 1.1 x 10^6 difference between the two groups, approaching significance with a resulting p-value of 0.0634.

Figure 5: *Trim24* knockout cells have increased cell number *in vitro*

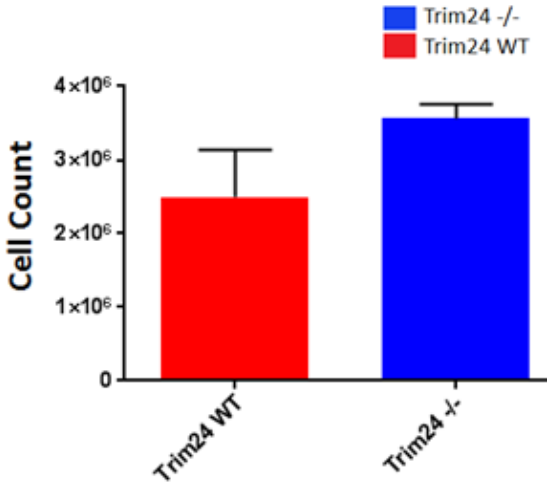

The y-axis represents total cell number per passage. The x-axis contains the categories for the control group (*Trim24* WT), and *Trim24* knockout (-/-).

Giemsa stains:

Giemsa stains aid in the visualization of morphological differences between hematopoietic cell types by not only making cellular features such as the nucleus more distinct, but by also providing unique staining patterns for specific cell types (such as light pink stain for erythroid cells). This staining provides the stark visual differences needed to manually distinguish between hematopoietic cell types, and enables manual enumeration of major hematopoietic cell populations. As such, this is frequently used as a method to measure blast counts

Figure 6: *Trim24* knockout cells show no difference in blast percentage

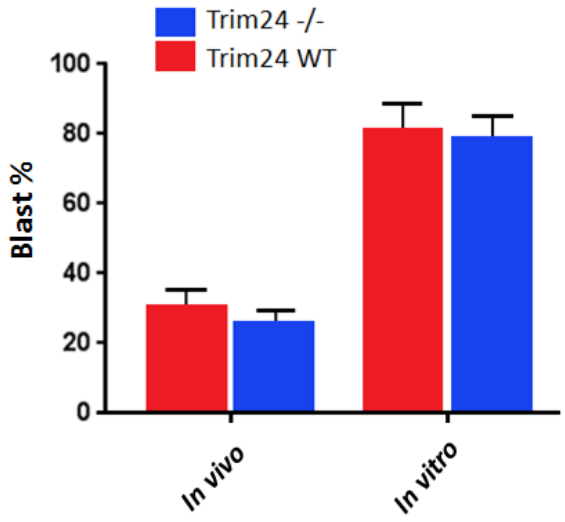

The y-axis represents the percentage of blast cells out of total cells enumerated via Giemsa staining. The x-axis represents the categories of *Trim24* knockout (blue) and *Trim24* wildtype (red) for both *in vivo* and *in vitro* experiments.

and biases towards the maturation of specific hematopoietic lineages. After performing Giemsa stains on *in vitro* generated *Trim24* knockout and wildtype AML, we measured no significant difference in blast counts, with the knockout group displaying a blast percentage of 79, and the wild-type group a percentage of 81.7, with a 0.85 p-value between the two groups. Additionally, a similar result was observed in subsequent *in vivo* assays, with the knockout group displayed a blast percentage of 26.3, and wild-type group a percentage of 31.3, with a 0.7 p-value between the two groups.

Primary transplant:

For better understanding the potential role *Trim24* may play in *in vivo* survival, we injected mice with *Trim24* knockout and wildtype leukemic cells generated *in vitro*, in an assay known as a primary leukemic transplant. The primary transplant revealed that mice with *Trim24* wildtype leukemia succumbed to the disease after an average of 49 days, whereas the mice with *Trim24* knockout leukemia succumbed after an average 70.5 days, with 50% censored at day 80. This yields a 21.5 day difference between the two groups, approaching statistical significance with a p-value of 0.0814. Two repeats of the primary transplant have so far failed to engraft.

Figure 7: Mice with *Trim24* knockout primary AML trend toward survival disadvantage

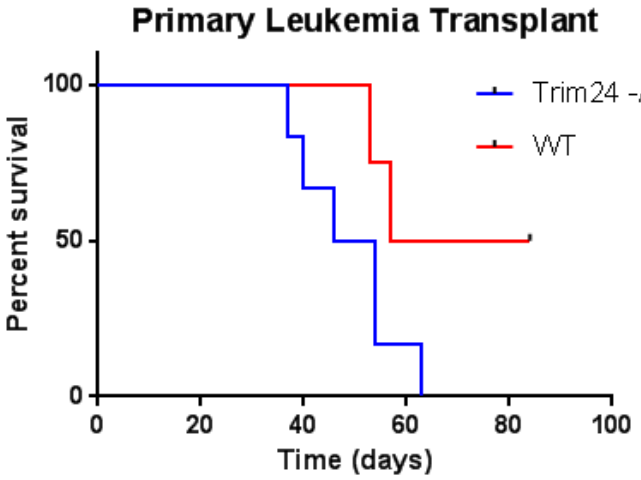

The y-axis represents the percentage of surviving patients in each group, while the x-axis represents the time of survival for mice after being injected with leukemic cells. *Trim24* knokcout group is represented in blue, whereas the *Trim24* wildtype group is represented in red.

Secondary transplant:

We next performed what is known as a secondary leukemic transplant by harvesting leukemic bone marrow cells from deceased mice in the primary transplant, and subsequently re-injecting them into immunocompromised mice. The purpose of such serial transplantations is to reveal long-term differences in the ability of a genotype to maintain a leukemic initiating cell (LIC) population, as such differences in self-renewal capacity are not always readily observable in primary transplants. The secondary transplants revealed a stark difference in the survival times between mice with *Trim24* wildtype leukemia and mice with *Trim24* knockout leukemia, with the knockout group displaying an average survival of 30.8 days, and the wildtype group displaying an average survival of 66.8 days, with 4 out of 6 censored at day 80. This gives a 36 day difference between the survival of the two groups, reaching statistical significance with a p-value of 0.0012. The secondary transplant was repeated, with the knockout group displaying an average survival of 45 days, and the wildtype group

Figure 8: Mice with *Trim24* knockout secondary AML show strong survival disadvantage.

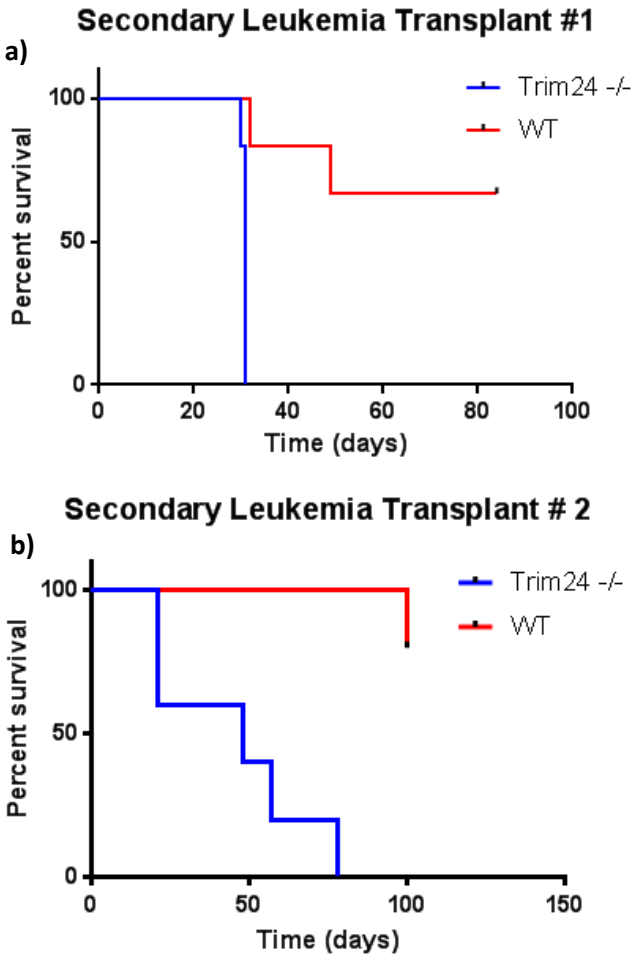

For both figure 8 a) and figure 8 b) the y-axis represents the percentage of surviving patients in each group, while the x-axis represents the time of survival for mice after being injected with leukemic cells. *Trim24* knokcout group is represented in blue, whereas the *Trim24* wildtype group is represented in red. Figure 8 a) represents the first iteration of the secondary transplant, whereas figure 8 b) represents a repeat.

displaying an average survival of 100 days, with 5 out of 6 censored at day 100. This gives a 55 day difference between the survival of the two groups, reaching statistical significance with a p-value of 0.0017.

Leukemic initiating cells:

To enumerate the rare cell population within leukemic tissue known as leukemic initiating cells (LICs), we performed antibody-staining and flow cytometry analysis on *Trim24* knockout and wildtype leukemic bone marrow from the transplantation experiments. The flow analysis revealed that mice with *Trim24* knockout leukemia have approximately six times as many leukemic initiating cells (GFP +, Sca1 -, lineage low, C-kit +, CD34 +, FcyR III/II -), with the knockout group having an average of approximately 870,000 leukemic initiating cells, and the wildtype group having an average of approximately 142,000 leukemic initiating cells. The exact difference is statistically significant, reaching a p-value of 0.0247.

Figure 9: Mice with *Trim24* knockout AML show 6-fold increase in leukemic initiating cells

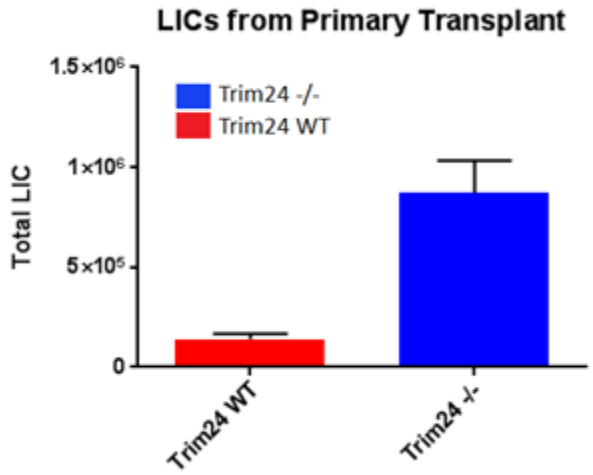

The y-axis represents the total number of leukemic initiating cells (LICs) enumerated per sample, while the x-axis contains the categories of *Trim24* wildtype leukemia (control) and *Trim24* knockout leukemia (*Trim24* -/-).

HOXA cluster expression:

To determine if altered HOXA cluster expression, a hallmark of *MLL*-fusion AML, varied between *Trim24* knockout and wildtype leukemic mice, we isolated RNA from our leukemic tissue, and performed qPCR. Analysis of the qPCR data revealed no significant difference in the expression of *HOXA9*, with *Trim24* knockout leukemic cells expressing 0.9 the amount of wildtype cells, with a non-significant p-value of 0.21. Additionally no significant difference in the expression of *MEIS1* (canonically expressed with the *HOXA9* cluster) was detected either, with *Trim24* knockout leukemic cells expressing 1.06-fold more than wildtype cells, with a non-significant p-value of 0.24.

Figure 10: Mice with *Trim24* knockout AML show no difference in HOXA cluster expression.

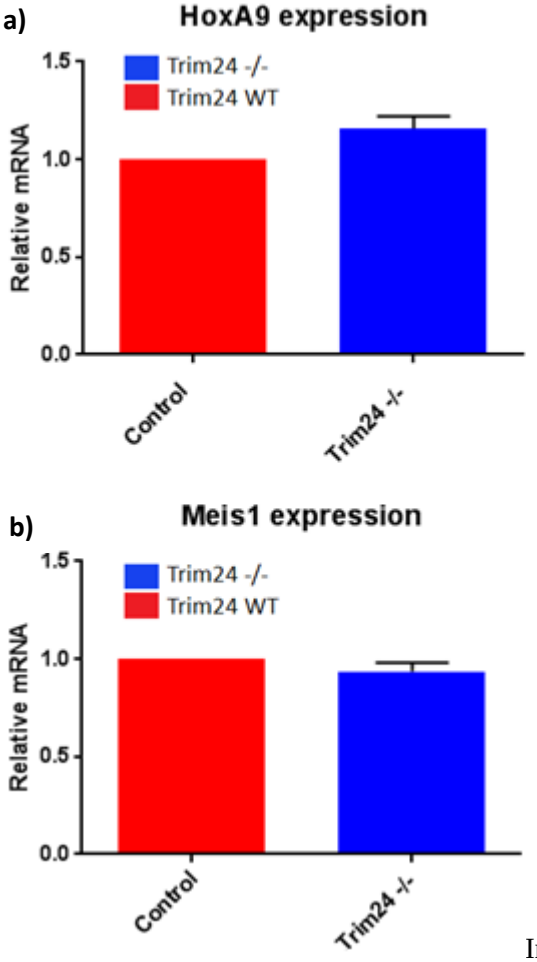

In both figure 10 a) and figure 10 b), the y-axis represents mRNA expression normalized to the control group (*Trim24* wildtype), while the x-axis contains the categories "Control" and "*Trim24* knockout". Figure 10 a) contains data for expression of *HOXA9*, while figure 10 b) contains data for expression of *MEIS1*.

Prognositc indicators:

To gather a more complete understanding of the putative clinical relevance of *TRIM24*, we first examined *TRIM24* mRNA expression in the context of patient prognostic markers. As can be seen in (figure 11 a), based on cytogenetic prognostic markers, *TRIM24* mRNA expression correlated with a favorable prognosis, with patients in the "Good" group expressing an average of 2784 reads per kilobase million (RPKM),

while patients in the "Intermediate" and "Poor" groups expressing an average of 1918 and 1703 RPKM of *TRIM24* mRNA respectively. After performing an ANOVA, the resulting p-value was less than 0.0001 in both cases when comparing "Good" to "Intermediate" or "Poor". No statistically significant difference was observed when comparing the "Intermediate" or "Poor" groups. Additionally, to determine if the observed association with a favorable prognosis could be attributed to altered mutation frequency, we next compared mutation rate with *TRIM24* mRNA expression per patient. Shown in (figure 11 b), *TRIM24* mRNA did not correlate with mutation rate in the TCGA AML dataset. Linear regression analysis resulted in a slope of 19.47, less than 1% of the mean *TRIM24* mRNA expression, and was not statistically significant, with a p-value of 0.115. The R-value (correlation coefficient) of the regression line generated was 0.015.

Figure 11: *TRIM24* mRNA correlates with favorable prognostic markers, independent of mutation rate.

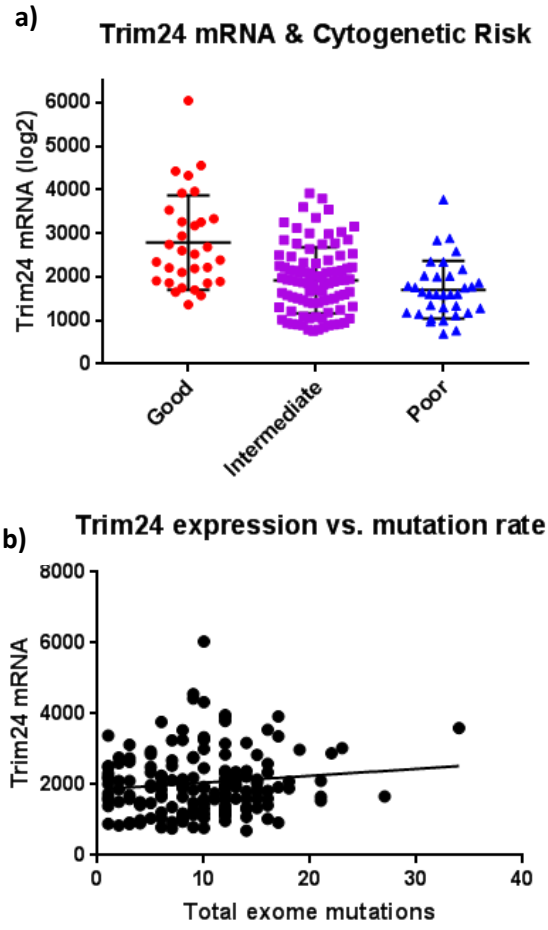

In figure 11 a) the y-axis represents *TRIM24* mRNA expression in reads per kilobase million (RPKM), while the x-axis contains three prognostic categories. In figure 11 b) the y-axis represents *TRIM24* mRNA expression in RPKM, while the x-axis represents total exome mutations per patient. All data in both figures were obtained from TCGA.

***TRIM24* mRNA expression by AML subtype:**

To assess the potential for subtype-specific biases of *TRIM24* expression, we examined the relationship between *TRIM24* expression and FAB subtype. As shown in (figure 12), the M3 FAB subtype displayed the highest mean *TRIM24* mRNA expression with an average of 2709 RPKM, reaching statistical significance when compared to M1, M4, and M5. Additionally, the M5 subtype displayed the lowest mean *TRIM24* mRNA expression with an average of 1173 RPKM, reaching statistical significance when compared to M0, M1, M2, and M3.

Figure 12: *TRIM24* mRNA expression varies across distinct AML subtypes

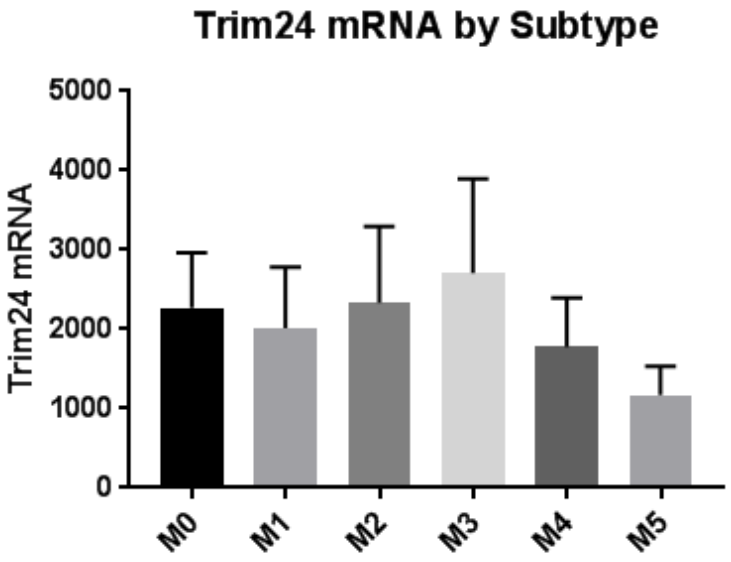

The y-axis represents *TRIM24* mRNA expression in RPKM, while the x-axis contains categories containing the six most-frequent subtypes of AML, according to the French-American-British (FAB) classification system.

***TRIM24* mRNA in HSCs & AML subtypes:**

As changes between hematopoietic stem cells (HSCs) and leukemic cells can be indicative of alterations beneficial to leukemic progression, we next examined *TRIM24* expression among five AML types and compared the mean expression of each group to that of HSCs. The data utilized for this analysis was obtained from the BloodSpot database. The BloodSpot database executes a batch-correction protocol on microarray data from various studies in order to make them comparable, enabling the comparison of leukemic data from the MILES study to hematopoietic data obtained from individual researchers. As can be seen in (figure 13), *TRIM24* expression is reduced among all five AML subtypes when compared to HSCs, all reaching statistical significance, each with a p-value less than 0.0001.

Figure 13: *TRIM24* mRNA is reduced in AML subtypes when compared to HSCs.

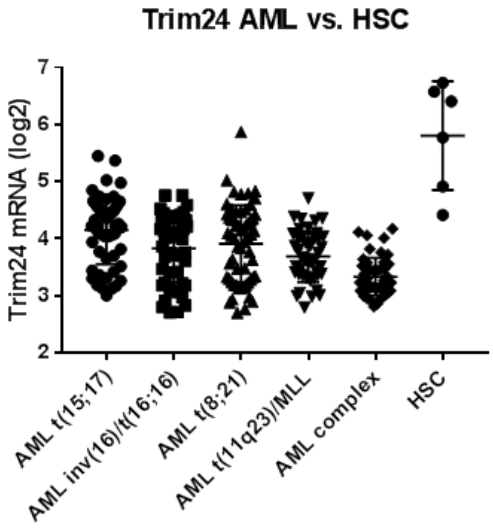

The y-axis represents *TRIM24* mRNA expression in RPKM, while the x-axis contains categories of five AML subtypes, and one category for hematopoietic stem cells (HSC). All data in this figure was obtained from the BloodSpot database.

TCGA patient survival:

To further evaluate *TRIM24*'s potential clinical relevance, we next examined survival trends between patients above mean *TRIM24* mRNA expression, and patients below mean *TRIM24* mRNA expression. As can be seen in (figure 14 a), patients with above mean *TRIM24* mRNA expression survived an average of 35.6 months, whereas patients below mean *TRIM24* mRNA expression survived an average of 19.6 months. The survival difference between these two groups is significant, reaching a p-value of 0.0003.

As can be seen in (figure 12), *TRIM24* expression correlated with the M3 FAB subtype of AML, which has a strongly favorable prognosis in comparison to the other FAB subtypes. To understand to what extent this association could be affecting the observed survival trend, we performed a separate survival analysis excluding all M3 patients (16 total). The resulting analysis (figure 14 b) shows that excluding M3 patients did not substantially affect survival, with a resulting p-value still significant at 0.0057. To further scrutinize the relationship between *TRIM24* mRNA expression and survival, our bionformatics collaborator (Yi Zhong) performed an independent survival analysis (figure 15) by removing arbitrary cut-offs such as "the mean", and instead used an optimized cutoff to define *TRIM24* high and low-expressing groups (see methods). This survival analysis was congruent with the prior two analyses, with *TRIM24* high expressing patients surviving longer than *TRIM24* low expressing patients, with a p-value of .0007.

Figure 14: *TRIM24* mRNA correlates with human survival across subtypes.

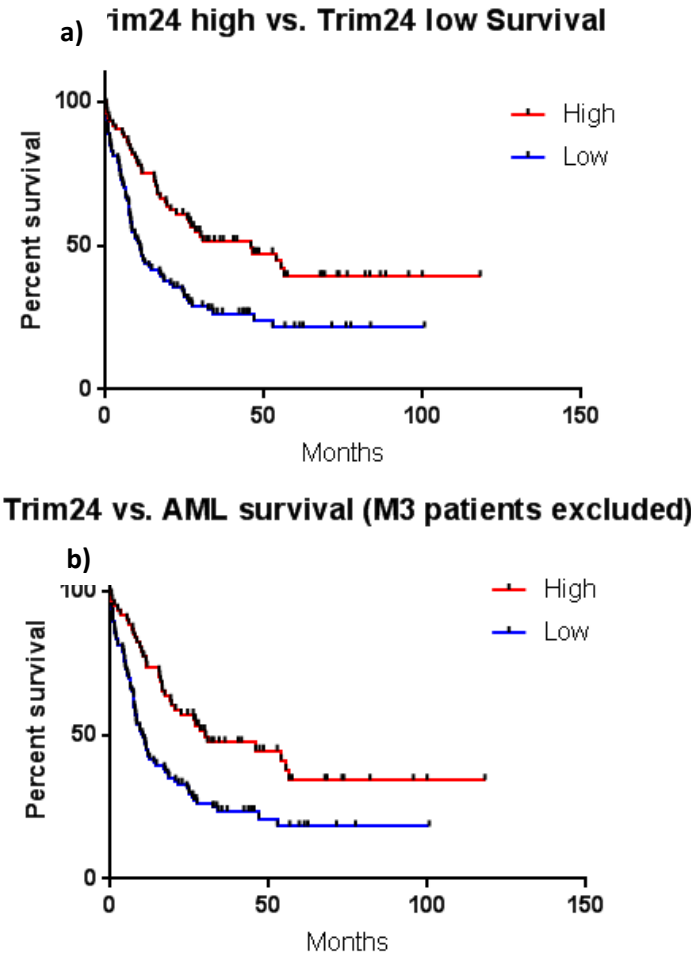

The y-axis represents percent of surviving patients while the x-axis represents months of patient survival post-diagnosis. *TRIM24* high expressing patients (red) and *TRIM24* low expressing patients (blue) were separated into their respective groups based on their *TRIM24* expression in comparison to the mean *TRIM24* expression of the group. All data was obtained from TCGA. Figure 14 a) and figure 14 b) differ only in that patients of the M3 subtype (16 in total) were excluded from the analysis in figure 14 b).

Figure 15: *Trim24* mRNA correlates with survival in independent, optimized-cutoff, ranked survival analysis.

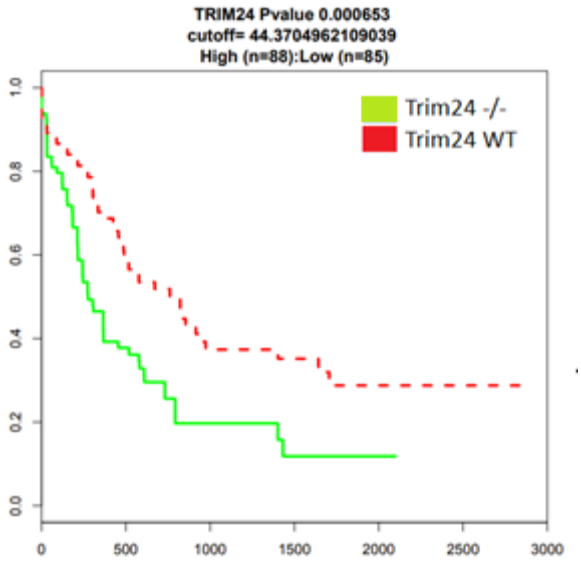

The y-axis represents the proportion of surviving patients in comparison to the total patients surviving (with 100% surviving represented by 1). The x-axis represents days survived post-diagnosis. *TRIM24* high expressing patients (red) and *TRIM24* low expressing patients (green) were defined by an optimzed cut-off algorithm. All data analyzed was obtained through TCGA. This figure is the reuslt of a collaboration with Yi Zhong.

TCGA Patient characteristics:

To determine if patient cell type biases were observed on the basis of *TRIM24* expression, we next examined *TRIM24* expression per patient in the context of various patient hematopoietic cell types. Demonstrated in (figure 16), *TRIM24* expression did not reaveal any statistically significant correlation with peripheral blood blast percentage (p-value 0.32), white blood cell count (p-value 0.11), basophil count (p-value 0.93), abnormal lymphocyte count (p-value 0.13), nor platet count (p-value 0.43). *TRIM24* did demonstrate a stastistically significant linear relationship with bone marrow blast percentage (p-value 0.02); however, the R-value (correlation coefficient) obtained from the linear regression analysis was 0.033, indicating an extremely weak linear relationship. The resulting slope (-8.3) is less than 0.41 % of the mean *TRIM24* mRNA expression.

Figure 16: *TRIM24* mRNA does not correlate with enumerated patient cell types.

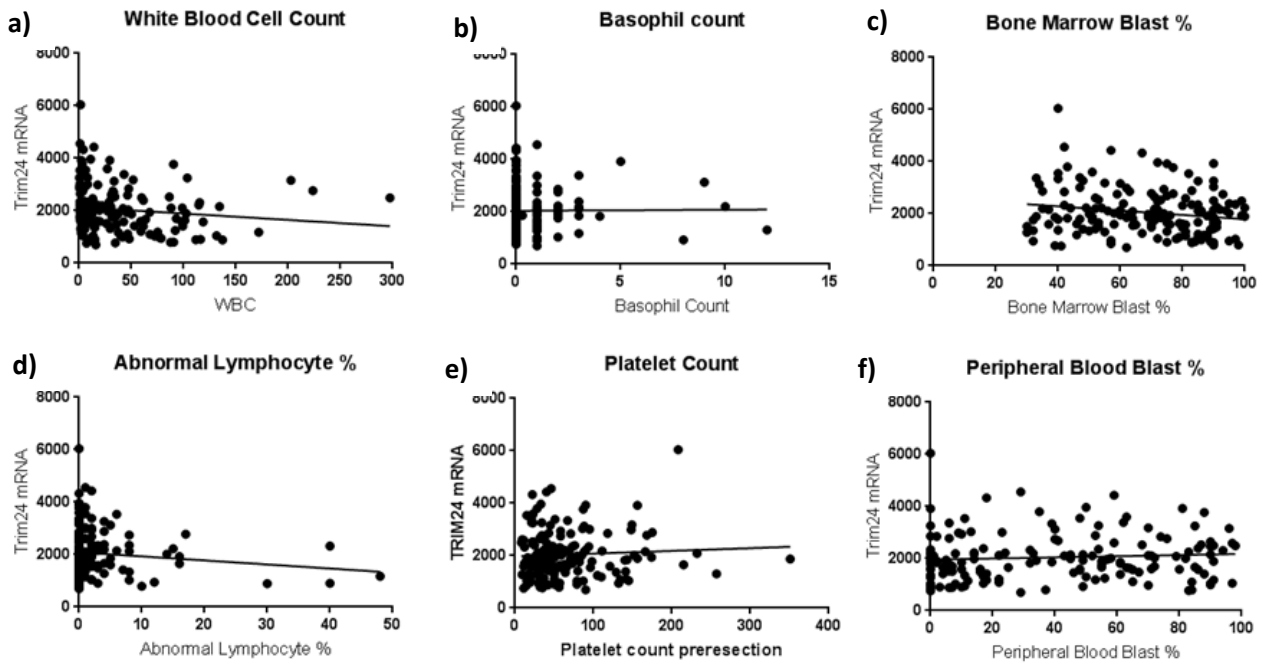

For figures 16 a) through figure 16 f), the y-axis represents *TRIM24* mRNA expression in RPKM while the x-axis represents numbers of white blood cells (WBC), basophil count, bone marrow blast percentage, abnormal lymphocyte percentage, platlet count, and peripheral blood blast percentage, respectively. All data in this figure was obtained through TCGA. The black line in each figure represents the slope generated from linear regression analysis.

TCGA HOXA cluster expression:

As with our *in vitro* and *in vivo* mouse AML samples, we next measured the co-expression between *TRIM24* and *HOXA9*, and *TRIM24* and *MEIS1* among all TCGA AML patients with mRNA sequencing data available. Statistically significant relationships were observed in both instances, with p-values of less than 0.0001; however, the associations were weak, with *HOXA9* co-expression yielding an R-value of 0.13, and *MEIS1* expression an R-value of 0.09. Repeating the analysis by examining *TRIM24* mRNA rank in comparison to *HOXA9* or *MEIS1* expression rank yielded a similar result, with R-values of 0.16 and 0.15 respectively.

Figure 17: *TRIM24* shows only weak association with HOXA cluster expression in TCGA.

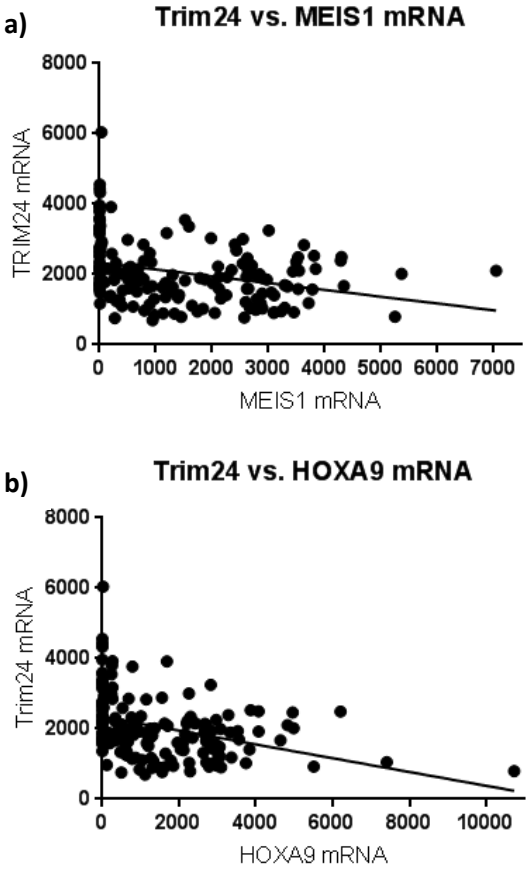

In both figure 17 a) and figure 17 b) the y-axis represents *TRIM24* mRNA expression in RPKM, while in 16 a) the x-axis represents *MEIS1* expression in RPKM, and in 16 b) the x-axis represents *HOXA9* expression in RPKM. The black line in each figure represents the slope generated from linear regression analysis.

Pathway Enrichment:

As the major gene cluster which facilitates LIC expansion in *MLL*-fusion AML was not strongly associated with *TRIM24* expression, we decided to next perform gene enrichment analysis on the co-expression data available from TCGA. Through collaboration with Yi Zhong, we obtained over 600 pathways significantly associated with *TRIM24* expression; however, many of these pathways encompassed various pathways involved in immune cell functions. As such, in table 1, we chose show the enrichment of 7 broad pathways which encompass many of the other pathways enriched in the *TRIM24* co-expression data. Additionally, at the bottom of table 1, we show the non-significant p-value for the association of a leukemic stem cell signature accepted for its prognostic value. This lack of an association with the canonical leukemic stem cell signature suggests a non-canonical survival mechanism may be responsible for *TRIM24*'s associations with survival (see discussion).

Table 1: Summarized pathway enrichment analysis

Pathway:	P-value	Correlation with Trim24:
GO_INNATE_IMMUNE_RESPONSE	1.3E-05	Negative
GO_REGULATION_OF_CYTOKINE_BIOSYNTHETIC_PROCESS	1.63E-05	Negative
GO_RESPONSE_TO_CYTOKINE	5.29E-05	Negative
GO_CYTOKINE_SECRETION	0.000198	Negative
GO_CHRONIC_INFLAMMATORY_RESPONSE	0.000429	Negative
GO_LEUKOCYTE_CHEMOTAXIS	0.000576	Negative
GO_LEUKOCYTE_ACTIVATION	0.006295	Negative
GENTLES_LEUKEMIC_STEM_CELL_UP	0.43149	Positive

The leftmost column displays the names for gene expression signatures from the Gene Ontology (GO) database. The middle column represents the p-value associated with their enrichment based on *TRIM24* mRNA expression, while the rightmost column displays nature of the association (i.e. positive vs. negative correlation). The first seven pathways listed represent pathways of interest for their statistically-significant associations with *TRIM24* mRNA, whereas the eighth pathway listed is a pathways with prognostic significance, noted in the literature for its association with leukemic stem cells.

Each of the pathways in Table 1 were evaluated for its correlation with survival in TCGA AML patients. Among these, leukocyte activation strongly associated with survival with a p-value of 0.0067 when comparing patients above and below median expression for the signature (figure 18).

Figure 18: Leukoctye activation signature negatively correlates with human survival.

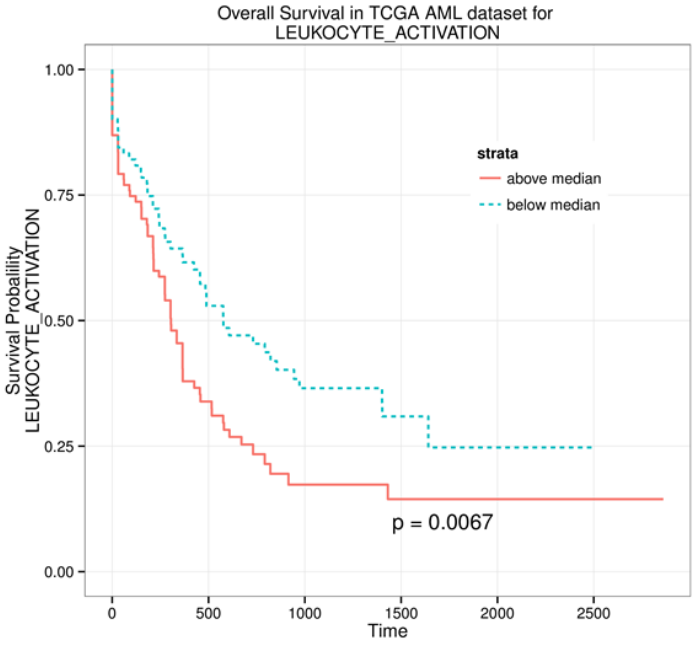

The y-axis represents percent of surviving patients while the x-axis represents days of patient survival post-diagnosis. Leukocyte activation high-expressing patients (red) and leukocyte activation low-expressing patients (blue) were separated into their respective groups based on their *TRIM24* expression in comparison to the median leukocyte activation expression of the group. All data in this figure was obtained from TCGA, and analyzed through software available through the BloodSpot database.

To determine if *TRIM24*'s negative association with the more mature M4 and M5 FAB subtypes (seen in figure 12) could account for *TRIM24*'s negative association with the leukocyte activation signature, we measured the co-expression of *TRIM24* with the "leukocyte activation" signature among solely M4 and M5 subtypes (excluding M0-M3 patients). Similar pathways, including the leukocyte activation signature, were still enriched among M4 and M5 patients.

Mutation enrichment by *TRIM24* mRNA expression:

To determine if differences in mutation patterns existed between *TRIM24* high and low expressing groups in TCGA, we compared the frequency of mutations for the top 12 most frequently mutated genes in AML between both groups. Defining high and low *TRIM24* expression based on the mean, or based on *TRIM24* expression greater or less than 1 standard deviation from the mean both yielded the same associative patterns between *TRIM24* mRNA expression and mutation frequency among the 12 genes (results in table 2).

Table 2: Enrichment of common mutations based on *TRIM24* mRNA expression

Above and below mean Trim24 mRNA expression:

	Mutation Rates:		Total Mutations	p-value	Association
	Trim24 High (68)	Trim24 Low (95)			
DNMT3A	0.18	0.29	40	*0.084*	**Negative**
FLT3	0.24	0.33	47	0.21	**Negative**
NPM1	0.21	0.35	47	***0.049**	**Negative**
TET2	0.07	0.11	15	0.4902	**Negative**
RUNX1	0.10	0.09	16	0.87	**Positive**
IDH2	0.06	0.13	16	0.153	**Negative**
TP53	0.04	0.12	14	*0.1074*	**Negative**
CEBPA	0.13	0.03	12	***0.0151**	**Positive**
IDH1	0.09	0.11	16	0.712	**Negative**
NRAS	0.03	0.11	12	*0.0672*	**Negative**
WT1	0.10	0.03	10	*0.0615*	**Positive**
KIT	0.04	0.03	6	0.6745	**Positive**

Above and below one standard deviation from the mean Trim24 mRNA expression:

	Mutation Rates:		Total Mutations	p - value	Association
	Trim24 High (25)	Trim24 Low (27)			
DNMT3A	0.24	0.48	19	*0.07*	**Negative**
FLT3	0.12	0.30	11	0.12	**Negative**
NPM1	0.08	0.48	15	***0.00142**	**Negative**
TET2	0.04	0.07	3	0.60	**Negative**
RUNX1	0.20	0.00	5	***0.01468**	**Positive**
IDH2	0.08	0.11	5	0.70	**Negative**
TP53	0.04	0.07	3	0.59	**Negative**
CEBPA	0.08	0.07	4	0.94	**Positive**
IDH1	0.04	0.15	5	0.19	**Negative**
NRAS	0.00	0.15	4	***0.0455**	**Negative**
WT1	0.04	0.00	1	0.29	**Positive**
KIT	0.04	0.037	2	0.95	**Positive**

***TRIM24* mRNA expression in non-AML TCGA datasets**:

In order to gather a more complete understanding of the biology behind loss of *TRIM24* expression in AML, we sought to find examples of loss of *TRIM24* correlating with poorer survival in other human malignancies. To this end, we analyzed survival based on *TRIM24* expression among all TCGA datasets possessing mRNA sequencing. From the data available, reduced *TRIM24* mRNA expression correlated with poorer survival in TCGA thyoma patients. Shown in (figure 19), patients below mean *TRIM24* mRNA expression displayed poorer survival when compared to patients above mean *TRIM24* mRNA expression, with a p-value of 0.0215 when comparing the two groups.

Figure 19: *TRIM24* mRNA expression correlates with survival in human thyoma patients

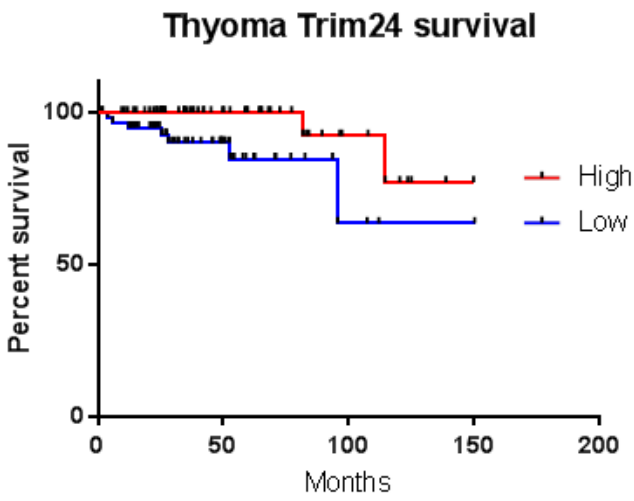

The y-axis represents percent of surviving patients while the x-axis represents months of patient survival post-diagnosis. *TRIM24* high expressing patients (red) and *TRIM24* low expressing patients (blue) were separated into their respective groups based on their *TRIM24* expression in comparison to the mean *TRIM24* expression of the group. All data was obtained from the thyoma dataset in TCGA.

To gather an understanding of the pathways putatively responsible for this survival relationship, we performed a gene enrichment analysis among *TRIM24* co-expressed genes in TCGA thyoma patients. Similar pathways to those enriched among the AML patients, including the leukocyte activation signature (p-value 0.00943), were enriched among genes negatively associated with *TRIM24* expression in thyoma patients.

TRIM24 Expression by Cell Type:

To first gain an understanding of how *TRIM24* could putatively affect hematopoiesis, we examined *TRIM24* mRNA expression by each major cell type in the hematopoietic differentiation hierarchy. This was accomplished by once again utilizing the batch-corrected data from the BloodSpot database. Demonstrated in figure 20, *TRIM24* mRNA is highest among HSCs, and decreases with increasing levels of cell maturation, with (BC, PMN, and MONO) displaying the lowest levels of *TRIM24* expression.

Figure 20: *TRIM24* mRNA expression is decreased in mature hematopoietic cell types.

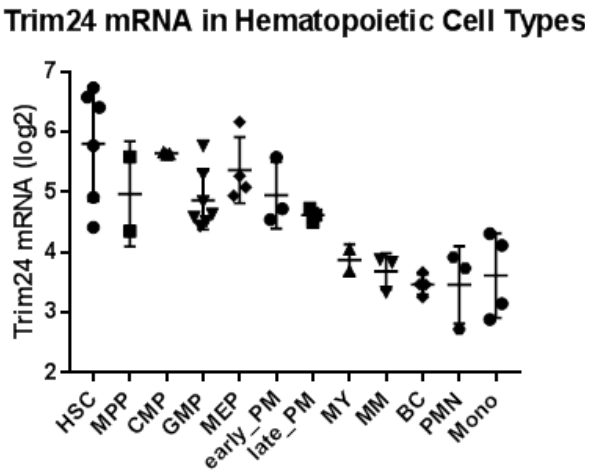

Figure 20 demonstrates that *TRIM24* mRNA expression is highest in hematopoietic stem cells (HSC) and lowest in differentiated cell types such as monocyte (Mono) and granulocytes (PMN). The y-axis demonstrates batch-corrected *TRIM24* mRNA expression values, while the x-axis contains all categories (cell types) examined. All batch-corrected mRNA exmamined in this figure was obtained from the BloodSpot database.

In an effort the role *Trim24* may play on major hematopoietic cell populations, we enumerated lymphocyte, neutrophil, and monocyte populations by utilizing side-scatter and forward-scatter metrics from flow cytometry experiments (see methods). As demonstrated in figure 21, in both *Trim24* knockout cells from the bone marrow and spleen, no difference in cell number was observed.

Figure 21: No difference in major cell populations between *Trim24* knockout and *Trim24* wildtype tissue.

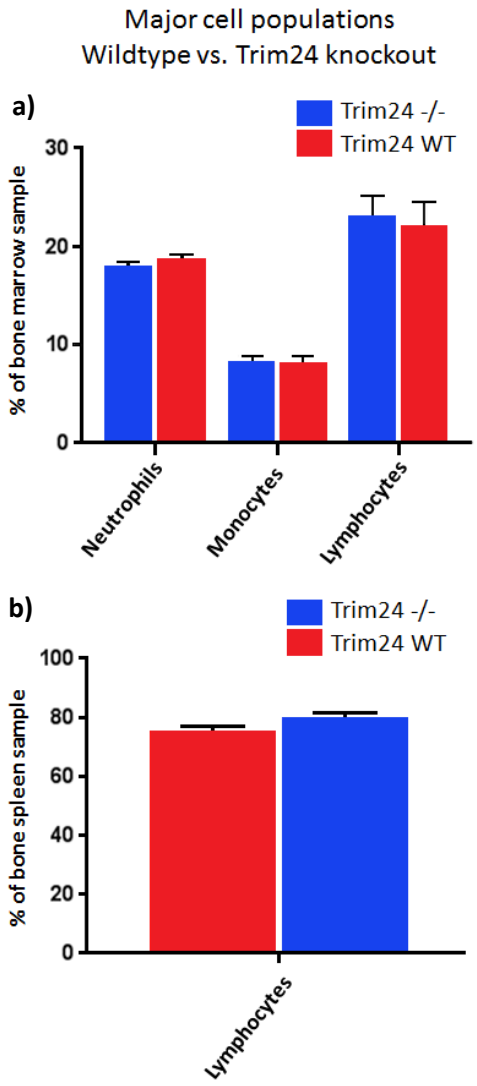

Both figures 21 a) and 21 b), no difference in major cell populations were detected between *Trim24* wildtype and knockout groups. In both figure 21 a) (bone marrow) and figure 21 b) (spleen) the y-axis represents the percentage of cells harvested from the tissue examined. In both figures, the x-axis contains the categories measured in each experiment, which are *Trim24* knockout (*Trim24* -/-) and *Trim24* wildtype (*Trim24* WT) groups for neutrophil, monocyte, and lymphocyte measurements. In figure 21 b), neutrophil and monocyte counts were unmeasurably low.

HOXA cluster expression in healthy bone marrow:

As with the leukemic bone marrow, we also used HOXA9 and *MEIS1* qPCR primers to gauge levels of HOX cluster expression. As shown in figure 22, no difference in HOX cluster expression was indicated by our qPCR.

Figure 22: No difference in HOXA cluster expression between *Trim24* knockout and *Trim24* wildtype healthy bone marrow

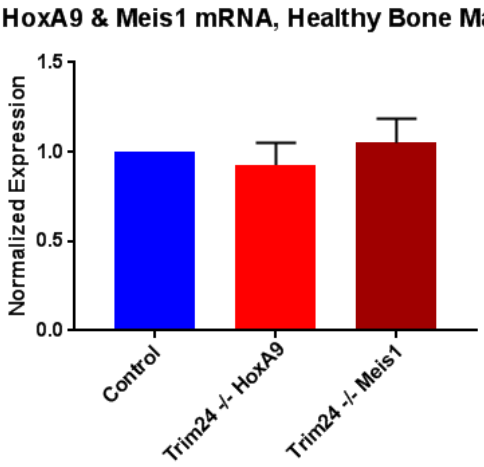

Figure 22 demonstrates no distinguishable difference in major HOXA cluster genes was observed between *Trim24* knockout and *Trim24* wildtype healthy bone marrow. the y-axis represents mRNA expression normalized to the control group (*Trim24* wildtype), while the x-axis contains the categories "Control", "*Trim24* knockout (-/-) *HOXA9*" and "*Trim24* knockout (-/-) *MEIS1*.

Effect of *Trim24* knockout on HSCs:

To determine if the HSC populations could be affected, fluorophore-conjugated antibodies were used to perform flow cytometry for the purpose of enumerating a population enriched for stem and progenitor cells, known as Lin-, Sca1+, Kit+ (LSK) cells. As shown in figure 23, the bone marrow of *Trim24* knockout mice (both in 12 week old and 6 month old mice) displayed no difference in LSK number when compared to wildtype mice from the same litter.

Figure 23: No difference in LSK number between *Trim24* knockout and *Trim24* wildtype healthy bone marrow.

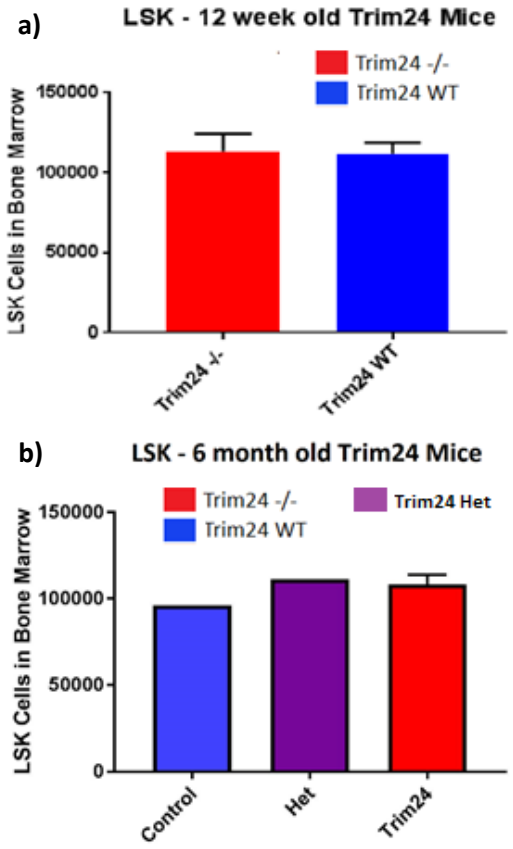

Figure 23 demonstrates no difference is observed for hematopoietic stem & progenitor cells (LSK) in the bone marrow of *Trim24* wildtype and knockout mice. For both figure 23 a) and figure 23 b), the y-axis represents the total number of LSKs in the tibia and femur bone marrow of mice. The x-axis contains all categories measured in the experiment, which include *Trim24* wildtype, *Trim24* heterozygous, and *Trim24* knockout mice.

Long-term competitive bone marrow reconstitution:

To gather a more complete understanding of any putative effects *Trim24* may have on normal hematopoiesis, we next performed a long-term bone marrow reconstitution (LTBMR) assay. Examining hematopoietic populations in the context of a LTBMR assay provides not only a temporal aspect by repeatedly measuring peripheral blood populations at regular intervals, but is also fundamentally different than observing populations in the steady state, as the replicative stress forced upon small populations to completely reform the bone marrow can cause otherwise unobservable phenotypes to arise. This assay provides great opportunities for observing biases towards cell maturation, but is also great for observing differences in self-renew capacity of HSCs. As shown in figure 24, the LTBMR assay revealed that mice reconstituted with *Trim24* knockout bone marrow displayed 2/3 the ability to reconstitute the bone marrow when compared to wildtype. An identical ratio was observed when comparing individual cell types. While our measurements have some level of variability, this ratio did not change over the 18 week span of the experiment.

Figure 24: *Trim24* knockout bone marrow shows mild reduction in reconstitution ability.

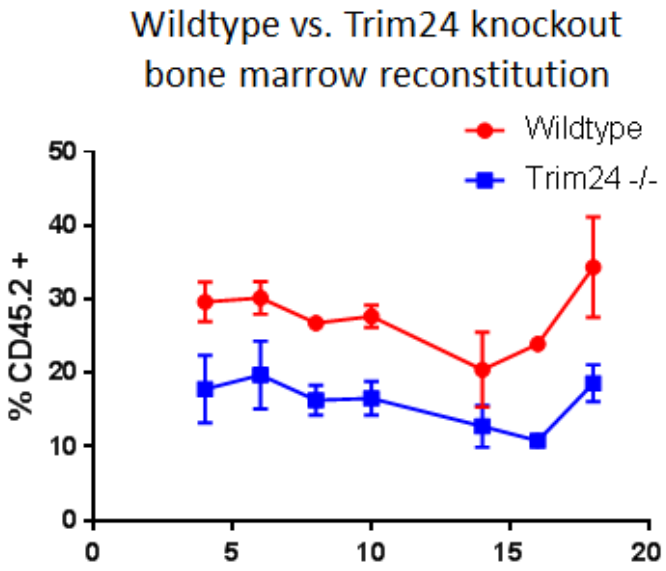

Figure 24 shows a roughly 2/3 difference in the ability of *Trim24* knockout (-/-) cells to reconstitute the bone marrow over a span of 18 weeks. The y-axis represents the percentage of CD45.2-positive cells observed per sample, which represents the reconstitution ability of each sample (see methods). The x-axis represents weeks post-injection of donor bone marrow following irradiation.

Discussion & Future Directions:

Trim24 knockout AML *in vitro*:

Colony formation assays are frequently utilized as a method to gauge the stemness and self-renewal capacity of cell populations. As is shown in figure 4, *Trim24* knockout *MLL-AF9* AML cells have an increased ability to form colonies *in vitro*. This phenotype indicates that, in comparison to wild-type cells, the *Trim24* knockout cell population has an increased number of stem-cell-like cells or an increased potential for self-renewal. As AML is primarily driven by malignant stem cells, measurements of *in vitro* self-renewal capacity have marked implications for predicting a genotype's effects on survival in an *in vivo* system. Accordant with the increased number of colonies, *Trim24* knockout leukemic cells also displayed an increased cell number per passage. To further examine *Trim24's* effects on self-renewal and differentiation in AML *in vitro*, Giemsa stains were performed on both the wildtype and knockout cells for the purpose of gauging levels of cell maturation present in each sample. As can be seen in figure 6, Giemsa staining revealed no detectable difference in blast cell counts between either cell population, nor showed visually-distinguishable biases for any specific mature hematopoietic cell type. Although the extent of cell maturation appears to be similar between the two genotypes, this alone is not contradictory to the colony formation data. Phenotypic differences may lie within the rare leukemic initiating cell (LIC) population, which may not be readily observable upon broadly examining cell maturation through Giemsa staining.

Trim24 knockout AML *in vivo*:

The limitations of *in vitro* assays led us to conduct similar *in vivo* assays for the purpose of better comprehending *TRIM24*'s potential relevance in AML. To this end, we performed primary leukemic transplants to assay the effect of *Trim24's* presence in AML. As shown in figure 7, no

significant survival difference was detected between wildtype and knockout groups; however, differences in survival frequently do not manifest themselves during the primary transplant. Often, phenotypic differences only evince themselves after serial transplantations, when the AML test groups are forced rely more heavily on LIC populations for sustained proliferation (86). After performing and repeating secondary transplants, mice with *Trim24* knockout AML displayed a marked decrease in survival (figure 8). This significant survival difference exclusive to the secondary transplant connotes, in parallel with the colony formation data, a disparity in maintenance of LICs. As with the *in-vitro* samples, we next measured broad levels of cell maturation through both Giemsa staining and Hemavet blood counts. In both cases, no detectable differences were observed between either genotype, further supporting the notion that *Trim24's* effects on AML may lie within the rare LIC population.

As the data available from *Trim24* knockout samples is characteristic of what would be observed from an increased self-renewal phenotype, we next enumerated the cell population postulated to be responsible - LICs. As can be seen in figure 9, fluorescent antibody labelling and subsequent flow cytometry revealed that mice with *Trim24* knockout AML displayed a 6-fold increase in LIC number. The quiescent nature of LICs confers a resistance to conventional therapeutics, which solely target proliferative pathways (34, 87, 88). Coupled with an elevated potential for self-renewal, LICs are widely accepted to possess the most potent effect on relapse and long-term survival of any known AML cell population (87, 88).

A paradigm in LIC maintenance for *MLL*-fusion driven AML is dysregulation of the HOXA gene cluster, which plays a central role in regulation of hematopoietic self-renewal in both malignant and healthy tissue. To determine if this mechanism of action could potentially account for *Trim24's* observed phenotypes, we performed qPCR on *Trim24* knockout and wildtype samples to measure the extent to which presence of *Trim24* affected expression of the key HOXA

cluster genes HOXA9 and *MEIS1*, both of which play roles in AML progression (89). Interestingly, in both leukemic bone marrow and *in vitro* samples, differences in the expression of neither were observed. While not indicative of any particular mechanism, these data suggest that *Trim24's* effect on the LIC population may be independent of HOXA cluster expression. More profoundly, this may indicate that *Trim24's* effects on AML may be largely independent of *MLL*-direct targets (including the HOXA cluster); however, further experimentation is required to explore this possibility. A substantial portion of therapeutic strategies for *MLL*-fusion AML operate through targeting these pathways, giving our current results encouraging potential for original clinical applications. The identification of a pathway novel with respect to AML LIC maintenance may illuminate previously unappreciated targets of clinical relevance, potentially opening up options for novel independent or combinatorial therapies.

***TRIM24* in AML TCGA data:**

Although experimentation in mice is generally an improvement over *in vitro* assays, limitations still exist. One such limitation is that merely a small fraction of drugs relevant in mice move past phase III clinical trials. To increase a study's probability of maintaining relevance in human trials, obtaining the maximum amount of available data from human tissue is of paramount importance. Accordingly, The Cancer Genome Atlas (TCGA) is a consortium involving participation from the NCI, NHGRI, and researchers from several hospitals, all aimed at comprehensively recording high-quality genomic information from human patients across 33 different cancer types. Along with recording next-gen sequencing data, an abundance of additional metrics were also recorded, enabling statistical association of mutation and expression data with patient characteristics. Among the samples available in this database, tissue from 173 adult AML patients had undergone both genomic and RNA sequencing.

We first used this information to search for associations between *TRIM24* expression and both patient prognosis and mutation status. This inspection revealed that high *TRIM24* mRNA expression correlated with both low risk molecular and cytogenetic markers (figure 11 a). Furthermore, mutation rate was not correlated with *TRIM24* mRNA expression (figure 11 b), suggesting *TRIM24*'s association with low risk prognosis markers is not an artifact arising from a lower mutation rate. Concordantly, a separate database holding a collection of leukemic and healthy hematopoietic microarray datasets (BloodSpot) demonstrated that *TRIM24* expression is reduced in AML when compared to HSCs (figure 13). This observation reinforces our hypothesis, as expression differences between HSCs and AML samples frequently represent alterations beneficial to leukemia. To further investigate *TRIM24*'s relevance in human AML, we next obtained mRNA sequencing data from TCGA AML patients, and compared survival between patients above and below mean *TRIM24* expression. As can be seen in figure 14a, patients with high *TRIM24* expression displayed a greatly increased survival, with a mean survival time 1.8 times greater than patients with low *TRIM24* expression. With the collaboration of Yi Zhong (a senior statistical analyst for the department of Epigenetics & Molecular Carcinogenesis at MD Anderson), we next performed a more thorough survival analysis by removing arbitrary cut-offs such as "the mean" (see methods) (figure 15). From this analysis, the survival difference remained strikingly prominent, yielding a p-value of 0.0007. A caveat to this result is our observation that high *TRIM24* expression is strongly associated with the M3 subclass of AML, which indisputably has the most favorable prognosis. However, after excluding all M3 patients, *TRIM24* expression still substantially correlated with survival (figure 14b), suggesting the observed survival trend is not merely an artifact of subtype-specific expression patterns. While the number of AML patients in TCGA is insufficient to perform a comprehensive multivariate analysis, all three survival

analyses correspond with both our data and original hypothesis that loss of *TRIM24* promotes the progression & aggressiveness of AML.

In line with our murine AML LIC and blast percentage data, metrics recorded by TCGA also demonstrate that *TRIM24* expression does not correlate with peripheral blood blast percentage, bone marrow blast percentage, platelet count, basophil count, nor white blood cell count (figure 16). As with the *in vitro* and *in* vivo data, the lack of a correlation between *TRIM24* expression and visually enumerable cell populations suggests that the survival trend in human patients could potentially be the result of altered characteristics of the LIC pool. Also in-line with our *in vitro* and *in vivo* data, an examination of co-expression between *TRIM24* and HOXA cluster genes in TCGA revealed no substantial association between the two (figure 17). This is directly in-line with the hypothesis that *TRIM24* is affecting survival through means other than canonical hematopoietic self-renewal pathways. To further investigate the validity of this theory, we next examined the co-expression in TCGA between *TRIM24* and a leukemic stem cell signature known for intensely correlating with patient survival, referred to as "Gentles leukemic stem cell up" in the Gene Ontology (GO) database (90). In congruency with the HOXA cluster expression data, *TRIM24* was not significantly correlated with the leukemic stem cell signature (Table 1). This result further supports the potentiality that the observed effects are a consequence of aberrations in a pathway novel with respect to AML progression.

To gather a more complete understanding of the pathways through which Trim24 could be affecting survival, we utilized co-expression data from TCGA to perform gene-enrichment analysis, yielding pathways enriched in both the top 1% of genes co-expressed with Trim24, and separately the top 1% of genes negatively co-expressed with Trim24. While not excluding the possibility, this analysis did not indicate that loss of Trim24 is negatively affecting human survival through other common oncogenic pathways. However, the gene enrichment analysis did reveal

that many immune-related pathways were associated with low *TRIM24* expression. While these immune regulatory pathways have no reported roles in AML, a re-examination of TCGA AML survival data revealed that one in particular, the leukocyte activation signature, negatively correlated with patient survival to a statistically significant extent (figure 18). Our collaborator, Yi Zhong, independently validated the signature's association with survival through ranked survival analysis utilizing an optimized cut-off (see methods).

A caveat worth mentioning is the observation that low *TRIM24* expression is associated with the M4 and M5 subclasses of AML (figure 12), both of which exhibit mature leukocytic features and poor survival. To evaluate this association as a potential artifact explaining the observed signature and corresponding survival, a separate gene enrichment analysis was performed exclusively on M4 and M5 patients. Consequently, the analysis revealed that *TRIM24* expression still negatively correlated with leukocyte activation, suggesting *TRIM24*'s association with the pathway is not merely an artifact of subtype-specific expression patterns.

In an effort to formulate a more complete picture of *TRIM24*'s participation in human malignancy, a broad examination of *TRIM24* expression among all TCGA data sets revealed that low *TRIM24* expression also correlated with poor survival in thyoma patients. Like the correlation of *TRIM24* expression and survival in AML patients, this observation is also unreported in the literature. Perhaps more relevant to our hypothesis, however, is the observation that the leukocyte activation signature was also found to be negatively associated with *TRIM24* expression in thyoma. This observation strongly bolsters the potential biological legitimacy of the statistical association between *TRIM24* and leukocyte activation in AML, as such a highly similar statistical anomaly occurring in two separate TCGA datasets is unlikely. These data, in combination with both previous reports of *TRIM24* expression associating with favorable bone marrow status in ALL and our concordant experimental results, strengthen the legitimacy of *TRIM24*'s statistical

association with survival in AML. This information altogether suggests that leukocyte activation may be the non-canonical pathway through which *TRIM24* expression exerts its observed effect on LICs in mice, and could potentially be the underlying reason why *TRIM24* expression correlates with survival in human patients.

The apparent biological connection between *TRIM24* and leukocyte activation should be, perhaps, unsurprising when examined in the context of the known role TRIM family members play in immunity. A number of TRIM family members have been demonstrated to participate in the regulation of interferon signaling, repression of retroviral elements, and cytokine transcript production (58, 59). These relationships provide rationale for *TRIM24*'s effect on AML LICs, when examined in the context of the HSC niche. The HSC niche is, in part, regulated by cytokines produced by surrounding immune cells, such as the production of IL-3 and GM-CSF by T-cells to support maintenance of HSCs (91-95). Correspondingly, genes comprising the "leukocyte activation" signature include several cytokines, as well as genes involved in their production and subsequent secretion. While many aspects of HSC maintenance are disrupted through aberrant regulation in AML, many of the same components affect the regulation of LICs(94, 96, 97).

While mechanistic studies are required to provide the information needed formulate a robust model, our current hypothesis is that *TRIM24* is indeed affecting AML leukemogenesis and progression by manipulating the expression of genes involved in the aforementioned "Leukocyte Activation" signature. More specifically, we hypothesize that loss of *TRIM24* expression alters the cytokine milieu in a cell-autonomous manner to support leukemic progression. In this hypothetical model (graphically described in figure 25), *TRIM24* represses a multitude of elements involved in immune regulation, including a collection of cytokines. Upon ablation of *TRIM24* expression, these cytokines, which partly comprise the leukocyte activation

Figure 25: Current hypothesis from data available

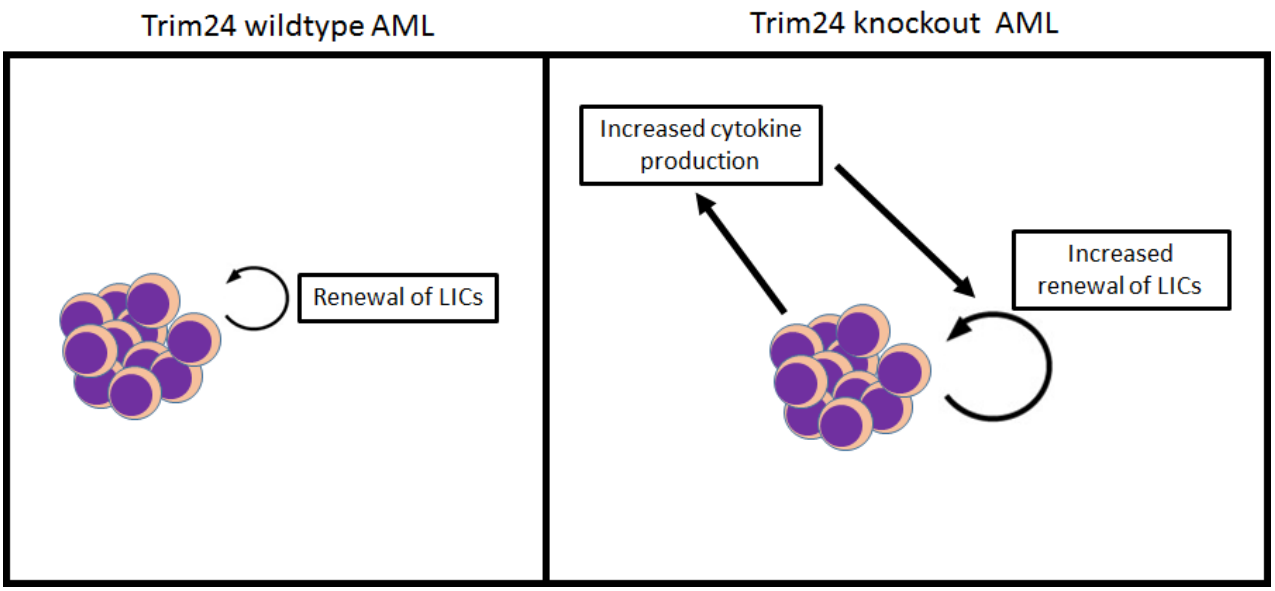

signature, become overexpressed in AML cells. Consequently, leukemic cells directly disrupt components of niche maintenance (such as IL-3 and GM-CSF signaling) and enforce positive-regulation of LIC niche characteristics that hinder patient survival. Although existing evidence is currently at an extremely preliminary stage, this hypothetical model outlines the rationale for further investigation of the relationship between *TRIM24* and leukocyte activation in AML.

***TRIM24* in normal hematopoiesis:**

With evidence suggesting a role for *TRIM24* in the regulation of LICs, we postulated that *TRIM24* may too regulate normal hematopoiesis in a similar fashion. While the literature describes roles for *TRIM24* in affecting immune cell expression, no reports to-date demonstrate a role for *TRIM24* in hematopoietic maintenance or maturation. Upon re-examining the BloodSpot datasets with particular focus on healthy hematopoietic cells, we observed that *TRIM24* expression is highest in HSCs and decreases with cell maturation, being lowest in myelocytes and monocytes. If *TRIM24* indeed negatively regulates leukocyte activation, this decrease in expression would be expected, so as to allow for the fulfillment of normal immune cell functions in mature hematopoietic cell types.

Paralleling our leukemic data, Giemsa staining of healthy *Trim24* knockout bone marrow and blood revealed no significant difference in cell maturation levels. Furthermore, a more intensive analysis of cell maturation was performed by utilizing flow cytometry to enumerate various hematopoietic lineages in the blood, spleen, and bone marrow, the results of which also failed to show any distinguishable difference between the two genotypes. Although no differences in cell number were observed, we sought to also directly enumerate the HSC populations of each genotype. To this end, long-term and short-term HSC populations were enumerated by once again performing flow cytometry analysis; however, after several repetitions, the results indicated no detectable difference between the two genotypes (figure 23). While these results are unsupportive of the hypothesis, differences in the ability to maintain a self-renewing stem cell population do not always manifest themselves from merely observing blood or bone marrow cell populations in the steady-state. The gold standard within this field for simultaneously comparing both self-renewal capacity and differentiation biases between two genotypes is the long-term competitive bone marrow reconstitution assay. This assay enables the comparison of each genotype's ability

to completely reconstitute the bone marrow and blood of lethally irradiated mice. By utilizing a variety of flow-cytometry antibodies, the extent to which each hematopoietic lineage is reconstituted can be individually measured. After recording the ratio of wild-type and *Trim24* knockout cell populations in the blood at 2-week intervals for 18 weeks, we sacrificed the mice and measured hematopoietic cell populations in the spleen and bone marrow. In all cases, the staining revealed no apparent bias for *Trim24* knockout cells to produce any specific cell-type. In contrast, a 2:3 ratio of total reconstitution ability was observed between *Trim24* knockout and wildtype samples (figure 24); however, while statistically significant, this difference in magnitude is mild. Repetition of this assay is needed to verify its results, as the observed discrepancy could merely be an artifact of improper sample preparation or test conditions. In line with this statement, a separate study reported no reconstitution advantage for *Trim24* knockout or wildtype bone marrow (98). Taken together, these data do not support our hypothesis that *TRIM24* plays an important role in normal hematopoiesis.

Future directions:

Before the commencement of further testing, we need to further optimize our *in vivo* protocols. In several attempts to repeat the primary leukemic transplants, *Trim24* wildtype leukemic bone marrow failed to engraft in immune-compromised mice. While the repeated successful engraftment of *Trim24* knockout leukemic bone marrow itself touts support of our hypothesis for *Trim24*'s role in leukemic progression, widespread results from the field demonstrate no issues with the engraftment of control cells. Without the development of leukemia within the control group, we cannot be certain all aspects of the protocol are being repeatedly properly. This issue must be addressed to not only provide repeats to enable clear statistical assessment of our observed data, but also to ensure no unforeseen confounding factors generate

artifacts within the data. Upon resolving this issue, further *in vivo* testing, such as additional survival analyses and measurement of cytokine levels, can progress.

To further evaluate the legitimacy of our gene enrichment analyses from TCGA data, we aim to use next-generation sequencing methods such as RNA-sequencing (RNA-seq) and chromatin immunoprecipitation sequencing (ChIP-seq) for the purpose of assessing the participation of pathways and individual genes through which *Trim24* could be exerting its effects in mice. Unlike the human TCGA data, testing a single sub-type of AML in highly inbred mouse strains removes the need for complex multivariate analyses. Furthermore, the capability of performing ChIP-seq in parallel with RNA-seq would enable for the cross-referencing of the resulting datasets, vastly limiting the potential regulators through which *Trim24* directly exerts its effects.

Beyond TRIM24's effects on gene expression, the protein's nuclear receptor interactions or E3 ubiquitin ligase activity could be responsible for our observed phenotypes. To address these possibilities, we intend to repeat our *in vivo* experiments with mice harboring non-synonymous mutations in the LXXLL motif of *Trim24* (responsible for nuclear receptor interactions). This assay should partly reveal the extent to which TRIM24's direct interaction with nuclear receptors effects *TRIM24*'s observed phenotypes in AML. In order to narrow down which receptor/s may depend on TRIM24 for nominal signaling in AML, monitoring the output of various nuclear receptors (with a key focus on retinoic acid receptor) should be experimentally assayed through qPCR of key targets for each receptor. Expanding on this assay by performing a non-biased method such as immunoprecipitation followed by mass spectrometry could yield a more complete understanding about the TRIM24 interactome, further guiding mechanistic investigations of *TRIM24* in AML. Although we do not anticipate *TRIM24*'s observed tumor suppressive activity in AML to be the result of P53 ubiquitination & degradation, we do expect that studying

TRIM24's RING domain in AML will provide useful insights into the mechanisms of action of Trim24 in AML. To this end, the E3 ubiquitin ligase activity of TRIM24 could also be responsible for many of the aforementioned phenotypes, potentially through targeting proteins other than P53. For this reason, assessing the effects of catalytically dead TRIM24 in an *in vivo* AML mouse model should yield valuable information relevant to the potential mechanisms and intermediary effectors through which *TRIM24* exerts its observed phenotypes.

Recent information from Dr. James Bradner's group has shed light on potential roles TRIM24's E3 ligase activity (RING domain) may play in AML (99). The group utilized a CRISPR-Scanning strategy to introduce mutations throughout the *TRIM24* locus in various acute leukemic cell lines, and determine which mutations were detrimental to the cell lines' progression. The results indicated that the cell lines examined (including the *MLL-AF9* expressing AML cell line, MOLM13) were dependent on an intact TRIM24 RING domain. While this information may at first appear contrary to the data presented in our study, *TRIM24* may play a balancing act in AML, which could account for the information presented in both studies. Similar to the fine balancing act *TRIM24* plays in hepatocellular carcinoma, overexpression and underexpression of *TRIM24* in AML could both have oncogenic consequences, albeit through different pathways. The stark difference in survival times between high and low expressing *TRIM24* patients may simply result from the varying molecular paths each group may take to achieve oncogenesis, potentially by leading to dissimilarities in disease progression or response to treatment.

This rationale leads to predictions for mutation patterns in AML. For example, if a subset of patients maintain high *TRIM24* expression for the oncogenic purpose of down-regulating P53, fewer *TP53* mutations should be observed, as the redundancy of such mutations will not aid the selection of an evolving malignancy. Conversely, low-expressing *TRIM24* patients would be expected to have a higher frequency of *TP53* mutations, as that would rescue the ability to reduce

P53 function lost with *TRIM24* expression. In accordance with this rationale, upon examining *TP53* mutations among TCGA AML patients, we indeed observe this trend, with 11 out of 13 *TP53* mutant patients displaying *TRIM24* expression below the mean. However, a sample size of only 13 *TP53* mutations is simply too small to give any statistical weight to this observation (p-value = 0.11). A larger sample size of mRNA expression and patient mutation data would be required to obtain the number of *TP53* mutants requisite for such an analysis. While this information is lightly supportive of *TRIM24* playing a balancing act in AML, a genome-wide mutation analysis in the context of *TRIM24* expression could provide further insight into which molecular landscapes coordinate with varying levels of *TRIM24* expression.

While current data does not support a role for *TRIM24* in normal hematopoiesis, a role may yet exist in a separate hematopoietic context. Given *TRIM24* theorized role in leukocyte activation, examining hematopoiesis within the context of chronic infection may yield differences in hematopoietic ability between *TRIM24* knockout and wildtype cells. Additionally, assaying the extent of leukocyte activation in *TRIM24* knockout and wildtype immune cells may yield insight into novel aspects of immunology.

Summary / Conclusion:

Overall, the cumulative data collected in this study supports our hypothesis that loss of *TRIM24* promotes the progression & aggressiveness of AML. While our data did not support the hypothesis that *TRIM24* plays an important role in normal hematopoiesis, this result is exciting when viewed within the context of clinical relevance. The lack of an apparent role for *TRIM24* in normal hematopoiesis suggests that AML therapies targeting the involved pathways may result in fewer negative side effects, potentially enabling a higher dosage and greater anti-leukemic effect than conventional treatments. Furthermore, our results lead us to hypothesize that

TRIM24's associations with survival are the result of a negative association between the expression of leukocyte activation and *TRIM24*. From the available data, we also theorize that this signature's correlation with poor prognoses is the result of altered regulation of leukemic initiating cells. Regardless of the true presence, or lack thereof, of a relationship between leukocyte activation and *TRIM24* expression, studying both in the context of AML progression will likely be a rewarding endeavor for providing a more comprehensive understanding of leukemogenesis and development of therapeutics. Ultimately, this study succeeded in providing a framework for guiding the continued research of *TRIM24* in AML.

Materials & Methods:

Cell culture: Unless otherwise specified, all cells in this study were cultured in RPMI 1640 with 2mm glutamine, cultured at 5% CO_2, 37 degrees in Corning Falcon® 10 cm dishes (REF 353003). All cell counts were performed by first spinning down harvested cells at 1500 RPM for 5 minutes at 4 degrees, and subsequently resuspending in PBS. 10 ul of this solution was then mixed with 10 ul of AOPI (Acridine orange & propidium iodide) stain and loaded onto a slide. Cells on the slide where then counted by a Cellometer® K2 machine.

Colony formation: All colony formation assays were performed with StemCell™ Methocult™ M3234 semisolid media (Cat# 03234), supplemented with 5 ng/ul IL-3, 5ng/ul, IL-6, 100 ng/ul SCF, and pen-strep antibiotic. Cultures were seeded with 5,000 cells in 2 mL Methocult in Corning Costar® 6-well plate (REF 3506). Plates were left in incubator with 5% CO_2 at 37 degrees for 10 days, at which point all plates were imaged with a Nexcelom Bioscience Celigo®-S to a resolution of 2 um per pixel. The resulting images were used to count colony types manually.

Storage of Cells: All cells were stored in freezing medium consisting of 90% FBS and 10% DMSO. Cells were harvested from cultures, washed in PBS, spun down at 1500 RPM for 5 minutes at 4 degrees, and subsequently re-suspended in freezing medium to a density of 4×10^6 cells per milliliter. The resulting suspensions were then aliquoted into Corning 2 mL cryovials (REF 430488), with 1.5 mL in each vial. The cryo-vials were next placed in a Nalgene cryo freezing container (Cat# 5100-0001), insulated with isopropanol, and placed in a -80 degree freezer. After allowing to freeze overnight, all vials were next transferred to boxes stored in liquid nitrogen.

qPCR: All RNA analyzed was harvested by following the TRIzol® protocol for harvesting RNA from suspension cells. Subsequently, cDNA copies of RNA were made by following the Bio-

Rad iScript™ Reverse Transcription Supermix protocol for generating cDNA. Per each well in our qPCRs, reaction mixtures were comprised of 5 ul SYBR Green master mix, 1ul forward primer, 1ul Reverse primer, 1 ul from 1:10 diluted cDNA stock, and 1 ul of DEPC water. The working stocks for each primer were 10 uM. All qPCRs were performed on a 7500 Fast Real-Time PCR System from Applied Biosystems. The machine was set to expose the sample to 95C for 5 minutes, then 40 cycles of 95C for 15s, 60C for 30s, and 72C for 30s. One final cycle was performed of 95C for 15s, 60C for 60s, 95C for 30s (during which melt curves were generated), and 60C for 15s. GAPDH was used as the reference gene for all qPCR experiments. All primers can be found in table 3.

Table 3 – primer sequences used in this study

Oligo Name	Length	Tm	Sequence
HOXA9 - F1	18	60.2	TTCCTGATGGCGTGATTA
HOXA9 - R1	18	54.5	CCTCTGTACTCTCCCTTG
HOXA9 - F2	18	57.3	ATTAATAGCGTGCGGAGT
HOXA9-R2	23	53.5	AAGTACAGTCACCTAATAAGTTG
MEIS1 - F1	23	56.8	AACCTCTATTCTCTTCTAATCCA
MEIS1 - R1	24	57.1	CATAATTCGTGTACCTTCTCTAAT
MEIS1 - F2	21	58.2	CAATGAAGATATAGCGGTGTT
MEIS1 - R2	20	58.7	CACTTGTATGGCTTGAATCA
GAPDH - F	19	61.3	GAAGGTGAAGGTCGGAGTC
GAPDH - R	20	60.8	GAAGATGGTGATGGGATTTC

Retroviral infection and bone marrow transformation : BOSC cells, previously frozen in freezing media, were thawed and allowed to recover for one passage in a Corning Falcon® 10 cm dish (REF 353003). BOSC cells were recovered and grown in DMEM with 10% FBS and pen-strep antibiotic. In the afternoon, 0.4 x 10^6 cells were plated in each well of a Corning Costar® 6-well plate (REF 3506) and allowed to grow overnight to approximately 70% confluence. Per well of cells, 6 ul of DNA:XtremeGene-9 was mixed with 1.6 ug of *MLL-AF9* plasmid, 1 ug of pCL-

Eco plasmid, and 94 ul of Opti-MEM. The reagents were mixed via pipette and allowed to incubate at room temperature for 15 minutes. 100 ul of the resulting mixture was added to each well of BOSC cells. 72 hours before transfection, donor mice were injected with 5-fluorouracil for the purpose of killing proliferating cells, and thus enriching donor bone marrow for hematopoietic stem and progenitor cells.

24 hours post-transfection, bone marrow from 8 – 12 week old mice was harvested, and plated in Corning Cellgro® DMEM (REF 10-013-CV) with 4ml per well and 2.5 million cells per well. 5ng / mL IL3, 5ng / mL IL6, and 100ng / mL SCF were added to the media, and cells were allowed to incubate at 37C for roughly 24 hours, to stimulate cell division.

48 hours post-transfection, BOSC culture supernatant (containing retrovirus) was harvested, and replaced with 2 mL of fresh DMEM. Viral supernatant was supplemented with the same mixture of cytokines described above, with the addition of 4ug / mL polybrene. Viral supernatant was then distributed equally among donor bone marrow cultures, which were subsequently spun at 2500 rpm for 90 minutes at 25C, then placed back in the incubator. 72 hours post-transfection, the collection and spinning of viral supernatant was repeated. The BOSC cells were harvested and run through flow cytometry analysis to determine transfection efficiency by measuring the percentage of GFP positive cells.

96 hours post-transfection, donor bone marrow cells were cultured in Corning Falcon® 10 cm dishes (REF 353003) with StemCell™ Methocult™ M3234 semisolid media (Cat# 03234), supplemented with 5 ng/ul IL-3, 5ng/ul, IL-6, 100 ng/ul SCF, and pen-strep antibiotic.

1-week post-transfection, donor bone marrow cells were harvested, spun down at 1500 rpm for 5 minutes at 4C, resuspended in 1mL of PBS, and placed on ice. A small fraction of these cells

were run through flow-cytometry to determine infection efficiency by measuring the percentage of GFP positive cells.

Primary leukemic transplant: To carry out primary leukemic transplants, NOD-SCID mice 8-12 weeks of age were injected through the tail vail with 100,000 GFP+ donor bone marrow cells from the transformation protocol. Mice were then monitored over the course of 100 days, and euthanized when displaying moribund leukemic symptoms, such as hunched posture, immobility, unkempt fur, short & rapid breathing, and closed or winced eyes. Blood, bone marrow, and spleens were all harvested after sacrificing leukemic mice. A leukemic diagnosis of each mouse was later confirmed by running bone marrow cells through flow cytometry to determine the percentage of GFP+ cells.

Secondary leukemic transplant: Secondary transplants were performed by harvesting leukemic bone marrow from mice which succumbed to leukemia in the primary transplant experiment as follows: the percentage of leukemic cells in the BM of primary recipients was determined by measuring the GFP percentage via flow cytometry. Based on this percentage, 100,000 GFP+ cells were subsequently injected into NOD-SCID mice 8 – 12 weeks of age. Mice were then monitored over the course of 100 days, and euthanized when displaying moribund leukemic symptoms. Blood, bone marrow, and spleens were all harvested after sacrificing leukemic mice.

Tail vein injection: Injections were carried out by placing mice in a restrainer specifically designed for tail vein injection, which holds the body of the mouse in place while exposing the tail. The tail was then warmed with a heat pad to induce vasodilation of the tail vein. Subsequently, a 28 gauge insulin needle was used to inject 200 ul of solution into mice. Such solutions varied on the experiment being conducted, but included bone marrow, leukemic cells,

and 5-fluorouracil (5FU). All 5FU injection solutions were prepared by mixing 5mg of 5FU with PBS for a final volume of 200 ul.

Euthanasia: In line with IACUC standards, mice were euthanized via CO_2 exposure in home enclosures with a flow rate of 30% displacement (1.8 liters) per minute until 1 minute after mice stop breathing (typically 6 minutes for adult mice). Our lab is approved to employ cervical dislocation or exsanguination as secondary euthanasia methods. For most mice, the thoracic cavity was immediately opened and the heart subsequently severed to not only ensure exsanguination as a secondary euthanasia method, but also to enable for the collection of large blood samples.

Harvesting of bone marrow: Immediately following euthanasia, mice were sprayed with 70% EtOH, and skin on the lower half of each animal was removed. Without damaging the ilium, the hind quarters were severed above the femur and immediately placed in ice-cold PBS. In a sterile hood, all muscle and ligaments were removed from the bone, and the femur and tibia were separated. A small incision was made on each end of the bones, and then PBS was flushed through them with a 28 gauge syringe, collecting all of the flow-through in a 1.5 mL tube. This process was repeated until visibly all bone marrow had been flushed from the bones. The solution with bone marrow was then spun at 2000 RPM at 4 degrees for 5 minutes, washed with PBS, subsequently spun at the same speed and resuspended in the desired volume for immediate usage, or frozen in freezing medium for future use.

Harvesting of spleen: Immediately following euthanasia, spleens were removed from the same mice from which bone marrow was harvested. The spleens were removed by extending the incision in the thoracic cavity (a remnant from the euthanasia protocol) downwards to expose organs in the abdomen. By gently moving intestines aside with forceps on the animal's left side,

the spleen was subsequently removed by using surgical scissors to separate the spleen from surrounding connective tissue. All spleens were immediately placed in ice cold PBS before future processing. For experiments in which sectioning of the spleen is intended, we halved the spleen, storing one half in 10% neutral buffered formalin (pH 6.8 – 7.2). The other half would then be forced through a 40 micrometer nylon cell strainer to separate the spleen into single cells. These cells would be washed in PBS, and were used for flow cytometry experiments, with excess cells being frozen in freezing medium.

Long-term competitive bone marrow reconstitution assay: CD45.1 C57/BL6 mice obtained from Charles River were committed to be recipients for the bone marrow transplant, and were thus irradiated with a lethal dose of 950 rads prior to receiving donor bone marrow. These mice were homozygous for the CD45.1 allele of CD45, so as to make any remnant cells distinguishable through flow cytometry from our test groups, which were homozygous for the CD45.2 allele. Donor bone marrow was harvested from *Trim24* knockout mice, *Trim24* wildtype mice, and CD45.1 homozygous C57/BL6. Separately, *Trim24* knockout and *Trim24* wildtype bone marrow were mixed with bone marrow CD45.1 C57/BL6 mice to obtain a 50:50 ratio of CD45.1 and CD45.2 cells (1.5×10^6 from each group). Both bone marrow mixtures (*Trim24* knockout / CD45.1 and *Trim24* wildtype / CD45.1) were injected into recipient mice, five for each group. Every 2 weeks for the span of 18 weeks, in each mouse the bone marrow reconstitution ability was measured by comparing the ability of *Trim24* knockout and *Trim24* wildtype cells to out-compete CD45.1 wildtype cells. The comparative ability of each genotype to reconstitute the blood is represented the ratio of CD45.1 and CD45.2 cells in each mouse, as measured by flow cytometry.

Geimsa stains: 50,000 cells in 50ul were first loaded onto a Thermo Scientific Cytoslide™ (REF 5991056) and subsequently adhered to the slide's surface through a cytospin protocol (800 rpm

centrifugation for 5 minutes). The resulting slides were placed in May-Grunwald stain for 7 minutes, then lightly rinsed with water. The slides were next placed in Giemsa stain, diluted 20-fold with distilled water, for 20 minutes. The slides were again lightly rinsed with water, and left face-up on a flat surface to air-dry. Blast percentages were counted by manually examining each slide under a microscope.

Harvesting Blood Post-mortem: After severing the heart, blood was allowed to pool in the bottom of the thoracic cavity for approximately 15 seconds. The pooled blood was then collected with a 1 mL pipet, and immediately transferred to a BD Microtainer® tube containing a K_2EDTA anti-coagulating solution (REF 365974). Each vial was either manually shaken or left on a rocker before analysis.

Harvesting Blood from Live Mice: All blood from live mice was collected by puncturing the facial vein with a 4mm lancet. 8 droplets of blood (approximately 100 – 200 ul) were collected from each mouse, directly in a BD Microtainer® tube containing a K_2EDTA anti-coagulating solution (REF 365974). Each vial was either manually shaken or left on a rocker before analysis.

Blood Counts: Blood collection tubes were placed into the HemaVet® hemacytometer, which takes 20 ul of blood from the sample and records numbers of leukocytes, neutrophils, lymphocytes, monocytes, eosinophils, basophils, erythrocytes, and thrombocytes.

Processing of Peripheral Blood: Immediately after harvest, blood samples were brought up to 10x the original volume with gibco® ACK lysis buffer (REF A10492-01). Samples were incubated with the buffer for 15 minutes at room temperature, periodically rocking the tubes manually. Each sample was then spun down at 2000 rpm at 4 degrees for 5 minutes, and all supernatant was removed. Each pellet was then resuspended in an additional 1 mL of ACK lysis buffer, and incubated for an additional 10 minutes at room temperature. Subsequently, 5 mL of

PBS was added to each sample and was then spun down at 2000 rpm at 4 degrees for 5 minutes, and all supernatant was removed.

Flow Cytometry: All flow cytometry was performed at the MD Anderson North Campus Flow Core. After harvesting or thawing the desired cells and obtaining the desired cell concentration, all flow samples were incubated in a primary antibody solution (concentrations & combinations can be seen in table 4) for 1 hour in the dark on ice. Each sample was subsequently spun at 1500 rpm at 4 degrees for 5 minutes. If a secondary antibody was required, it was instead resuspended in the secondary antibody solution and incubated for 1 hour in the dark on ice, otherwise each sample was resuspended in 300 ul of PBS with 2% FBS. Each sample was then passed through a 35 um nylon cell strainer and moved to a Falcon® 5 mL round bottom tube on ice. All samples and controls were then given to the core and run on a Gallios flow cytometer.

Table 4 – antibody combinations & concentrations

LSK stain					
Marker:	Lineage	Sca1	Kit	FLT3	CD34
Color:	PE	PE-Cy&	FITC	Biotin	AF647
Dilution:	100	100	50	100	25

Granulocyte, B-cell, Erythroid, and T-cell staining						
Marker:	GR1	Mac1	CD19	Ter119	CD4	CD8
Color:	APC	Ax647	PerCy5.5	PeCy7	PE	PE
Dilution:	100	100	100	100	100	100

LIC stain:						
Marker:	Sca1 -	C-kit +	Fcy R III/II -	CD34 +	Lineage-low	GFP +
Fluorophore:	Pe - Cy7	PerCP - Cy5.5	Biotin	AF647	PE	
Dilution:	100	50	100	25	100	
Secondary antibody:			Streptavadin - BV 421			
Dilution:			100			

Long-term competetive bone marrow reconstitution assay:								
Marker:	GR1	Mac1	CD19	Ter119	CD4	CD8	CD45.1	CD45.2
Color:	APC	Ax647	PerCy5.5	PeCy7	PE	PE	FITC	Biotin
Dilution:	100	100	100	100	100	100	100	100
Secondary antibody:								Pac-blue
Dilution:								100

TCGA data: All TCGA data was downloaded through the cBioPortal, an online website dedicated to providing access to annotated TCGA results, as well as providing a query function to download data relevant to only genes of interest. These data included sequencing data from 200 adult AML patients, with 173 of these patients also having mRNA sequencing recorded. Metrics analyzed in this study include cell-type numbers, patient survival, patient prognosis, and patient classification, and expression of individual genes.

***TRIM24 mRNA* association with quantitative patient metrics:** For each quantitative (non-categorical) variable recorded by TCGA examined in this study, linear regression analysis was performed with *TRIM24* mRNA expression, providing correlation coefficients and slopes of regression. The p-values generated represent the statistical significance of the observed slopes being non-zero.

***TRIM24* mRNA survival analysis:** *TRIM24*'s correlation with overall survival in human AML patients from the TCGA database was calculated by first separating patients into two groups based on *TRIM24* mRNA expression. Patients with *TRIM24* mRNA expression above the mean were defined as *TRIM24* high expressing patients, and those expressing below mean expression were defined as *TRIM24* low expressing patients. Next, survival curves were generated for each group, the differences between which were statistically evaluated by utilizing a Log-rank (Mantel-Cox) test. The same protocol was utilized when examining *TRIM24*'s association with survival in all other TCGA datasets. The same protocol was also followed upon evaluating *TRIM24* survival in the absence of FAB M3 subtype patients (16 excluded in total). The mean *TRIM24* mRNA expression was re-calculated, and the survival between *TRIM24* high and low expressing patients was re-evaluated.

Our collaborator Yi Zhong performed an independent survival analysis, in which arbitrary cutoffs (such as mean) were not used. Instead, he utilized an optimized cutoff value, in which a program repeatedly performed multiple survival analyses to find a cutoff which associates with survival to the greatest magnitude. The rationale behind this method is to provide a cut-off value which holds more biological relevance than any arbitrarily-chosen value. This has the potential to provide more biologically relevant gene enrichment analyses by separating patients based on that same cut-off value.

***TRIM24* mRNA mutation analysis:** The top 12 most frequently mutated genes in TCGA AML patients (as determined by cBioPortal annotation of patient exome sequencing) were examined for mutation enrichment based on *TRIM24* mRNA expression. Mutation count for each gene among *TRIM24* high and low expressing patients were tallied and compared, the numbers from which were statistically evaluated by utilizing Fisher's exact test.

***TRIM24* mRNA association with cytogenetic risk:** *TRIM24*'s association with cytogenetic risk was evaluated by plotting *TRIM24* mRNA expression for all patients within the 3 TCGA-annotated cytogenetic risk groups, "Good", "Intermediate", and "Poor". The resulting information was analyzed statistically by performing a 1-way ANNOVA with Tukey's multiple comparison test. The multiple comparison test compared the mean of each group, to the mean of each remaining group individually, providing an adjusted p-value for the difference obtained in each comparison.

***TRIM24* by French-American-British (FAB) classification of AML:** The association of *TRIM24* mRNA with AML FAB subtypes was examined by comparing the mean *TRIM24* mRNA expression of each group, and subsequently performing a 1-way ANNOVA with Tukey's multiple comparison test. The multiple comparison test compared the mean of each group, to the mean of

each remaining group individually, providing an adjusted p-value for the difference obtained in each comparison.

Gene enrichment analysis: Preliminary gene enrichment analyses were performed by obtaining *TRIM24* co-expression data for the entire genome, provided by cBioPortal. From the genomic co-expression data, we formulated a list of the top 1% of genes in the genome co-expressed with *TRIM24* mRNA, and a separate list of the top 1% of genes negatively co-expressed with *TRIM24* mRNA. These lists were then separately run through online PANTHER software, which compares the number of genes in each GO-annotated pathway in your list, and evaluates the statistical difference of this number with the expected number of genes (under the assumption of random distribution). The PANTHER software was chosen both for its ease of access, and recent update of GO pathways (updated monthly). For all results, this protocol was performed unless otherwise specified.

Our collaborator, Yi Zhong, independently performed a more intensive gene enrichment analysis. This involved utilizing an algorithm which provides a gene enrichment score for each GO pathway for each patient. Next, a simply t-test was performed to determine if these gene enrichment values varied significantly between *TRIM24* high and low groups, defined by the same cut-off obtained in Yi Zhong's survival analysis.

***TRIM24* mRNA in normal hematopoietic cell types:** *TRIM24*'s association with specific hematopoietic cell types was evaluated by statistically analyzing the relationship between *TRIM24* mRNA expression and corresponding cell type category. These information were obtained through a database known as BloodSpot, which compiles microarray data from multiple studies, and uses an algorithm to provide batch corrections to all data, to make the data comparable between all studies in the database. The statistical relationship between *TRIM24* mRNA and cell

type was computed by performing a 1-way ANNOVA with Tukey's multiple comparison test. The multiple comparison test compared the mean of each group, to the mean of each remaining group individually, providing an adjusted p-value for the difference obtained in each comparison.

***TRIM24 mRNA* in AML and HSCs:** Differences in *TRIM24* expression between 5 different AML subtypes and normal hematopoietic stem cells (HSCs) were statistically evaluated by performing a 1-way ANNOVA with Tukey's multiple comparison test on the *TRIM24* microarray data from each group. The multiple comparison test compared the mean of each group, to the mean of each remaining group individually, providing an adjusted p-value for the difference obtained in each comparison. The microarray mRNA data was obtained through a database known as BloodSpot, which compiles microarray data from multiple studies, and uses an algorithm to provide batch corrections to all data, to make the data comparable between all studies in the database.

Bibliography:

1. Lux CT, Yoshimoto M, McGrath K, Conway SJ, Palis J, Yoder MC. 2008. All primitive and definitive hematopoietic progenitor cells emerging before E10 in the mouse embryo are products of the yolk sac. *Blood* 111: 3435-8
2. Kim CH. 2010. Homeostatic and pathogenic extramedullary hematopoiesis. *J Blood Med* 1: 13-9
3. Abkowitz JL, Catlin SN, McCallie MT, Guttorp P. 2002. Evidence that the number of hematopoietic stem cells per animal is conserved in mammals. *Blood* 100: 2665-7
4. Catlin SN, Busque L, Gale RE, Guttorp P, Abkowitz JL. 2011. The replication rate of human hematopoietic stem cells in vivo. *Blood* 117: 4460-6
5. Seita J, Weissman IL. 2010. Hematopoietic stem cell: self-renewal versus differentiation. *Wiley Interdiscip Rev Syst Biol Med* 2: 640-53
6. Morrison SJ, Weissman IL. 1994. The long-term repopulating subset of hematopoietic stem cells is deterministic and isolatable by phenotype. *Immunity* 1: 661-73
7. Cordeiro Gomes A, Hara T, Lim VY, Herndler-Brandstetter D, Nevius E, Sugiyama T, Tani-Ichi S, Schlenner S, Richie E, Rodewald HR, Flavell RA, Nagasawa T, Ikuta K, Pereira JP. 2016. Hematopoietic Stem Cell Niches Produce Lineage-Instructive Signals to Control Multipotent Progenitor Differentiation. *Immunity* 45: 1219-31
8. Suda J, Suda T, Ogawa M. 1984. Analysis of differentiation of mouse hemopoietic stem cells in culture by sequential replating of paired progenitors. *Blood* 64: 393-9
9. Trumpp A, Essers MA, Steinmetz LM, Suda T, Suda J, Ogawa M. 1984. Disparate differentiation in mouse hemopoietic colonies derived from paired progenitors. *Nat Cell Biol* 81: 2520-4

10. Velten L, Haas SF, Raffel S, Blaszkiewicz S, Islam S, Hennig BP, Hirche C, Lutz C, Buss EC, Nowak D, Boch T, Hofmann WK, Ho AD, Huber W. 2017. Human haematopoietic stem cell lineage commitment is a continuous process. 19: 271-81

11. Mulder E. 1974. Counting cells in human bone marrow. *Am J Clin Pathol* 61: 199-202

12. Morrison SJ, Scadden DT. 2014. The bone marrow niche for haematopoietic stem cells. *Nature* 505: 327-34

13. Scadden DT. 2014. Nice neighborhood: emerging concepts of the stem cell niche. *Cell* 157: 41-50

14. De Kouchkovsky I, Abdul-Hay M. 2016. 'Acute myeloid leukemia: a comprehensive review and 2016 update'. *Blood Cancer J* 6: e441

15. Bowman RL, Busque L, Levine RL. 2018. Clonal Hematopoiesis and Evolution to Hematopoietic Malignancies. *Cell Stem Cell* 22: 157-70

16. Yao JC, Link DC. 2017. Concise Review: The Malignant Hematopoietic Stem Cell Niche. *Stem Cells* 35: 3-8

17. Hoggatt J, Kfoury Y, Scadden DT. 2016. Hematopoietic Stem Cell Niche in Health and Disease. *Annu Rev Pathol* 11: 555-81

18. Asai T, Liu Y, Bae N, Nimer SD. 2011. The p53 tumor suppressor protein regulates hematopoietic stem cell fate. *J Cell Physiol* 226: 2215-21

19. McKenna SL, Cotter TG. 1997. Functional aspects of apoptosis in hematopoiesis and consequences of failure. *Adv Cancer Res* 71: 121-64

20. Domen J, Cheshier SH, Weissman IL. 2000. The role of apoptosis in the regulation of hematopoietic stem cells: Overexpression of Bcl-2 increases both their number and repopulation potential. *J Exp Med* 191: 253-64

21. 2016. Surveillance, Epidemiology, and End Results (SEER) Program: Populations - Total U.S (1969-205) Linked to County Attributes - Total U.S., 1969-2015 Counties. National Cancer Institute

22. Mark Iscoe KJN, Gabriel Ghiaur, B. Douglas Smith, Christopher Gocke, Richard J Jones. 2016. The Cell of Origin in NPM1 Positive Acute Myeloid Leukemia (AML) is Prognostic. *Blood* 128

23. Krivtsov AV, Figueroa ME, Sinha AU, Stubbs MC, Feng Z, Valk PJ, Delwel R, Dohner K, Bullinger L, Kung AL, Melnick AM, Armstrong SA. 2013. Cell of origin determines clinically relevant subtypes of *MLL*-rearranged AML. *Leukemia* 27: 852-60

24. George J, Uyar A, Young K, Kuffler L, Waldron-Francis K, Marquez E. 2016. Leukaemia cell of origin identified by chromatin landscape of bulk tumour cells. 7: 12166

25. Arber DA, Orazi A, Hasserjian R, Thiele J, Borowitz MJ, Le Beau MM, Bloomfield CD, Cazzola M, Vardiman JW. 2016. The 2016 revision to the World Health Organization classification of myeloid neoplasms and acute leukemia. *Blood* 127: 2391-405

26. Drexler HG. 1987. Classification of acute myeloid leukemias--a comparison of FAB and immunophenotyping. *Leukemia* 1: 697-705

27. Slany RK. 2009. The molecular biology of mixed lineage leukemia. *Haematologica* 94: 984-93

28. Saultz JN, Garzon R. 2016. Acute Myeloid Leukemia: A Concise Review. *J Clin Med* 5

29. Jordan CT. 2007. The leukemic stem cell. *Best Pract Res Clin Haematol* 20: 13-8

30. Vasanthakumar A, Godley LA. 2014. On the origin of leukemic species. *Cell Stem Cell* 14: 421-2

31. Haase D, Feuring-Buske M, Konemann S, Fonatsch C, Troff C, Verbeek W, Pekrun A, Hiddemann W, Wormann B. 1995. Evidence for malignant transformation in acute

myeloid leukemia at the level of early hematopoietic stem cells by cytogenetic analysis of CD34+ subpopulations. *Blood* 86: 2906-12

32. Manaloor EJ, Neiman RS, Heilman DK, Albitar M, Casey T, Vattuone T, Kotylo P, Orazi A. 2000. Immunohistochemistry can be used to subtype acute myeloid leukemia in routinely processed bone marrow biopsy specimens. Comparison with flow cytometry. *Am J Clin Pathol* 113: 814-22

33. Kyle RA. 1966. Acute myelocytic (granulocytic) leukemia: current therapy. *Minn Med* 49: 1715-7

34. Dombret H, Gardin C. 2016. An update of current treatments for adult acute myeloid leukemia. *Blood* 127: 53-61

35. Chen Y, Kantarjian H, Wang H, Cortes J, Ravandi F. 2012. Acute promyelocytic leukemia: a population-based study on incidence and survival in the United States, 1975-2008. *Cancer* 118: 5811-8

36. Nowak D, Stewart D, Koeffler HP. 2009. Differentiation therapy of leukemia: 3 decades of development. *Blood* 113: 3655-65

37. Kolb EA, Gamis AS, Smith MA, Gerhard DS, Meshinchi S, Greenblatt SM, Nimer SD. 2014. Chromatin modifiers and the promise of epigenetic therapy in acute leukemia. *Nat Med* 28: 1396-406

38. Bolouri H, Farrar JE. 2018. The molecular landscape of pediatric acute myeloid leukemia reveals recurrent structural alterations and age-specific mutational interactions. 24: 103-12

39. Li Y, Xu Q, Lv N, Wang L, Zhao H, Wang X, Guo J, Chen C, Li Y, Yu L. 2017. Clinical implications of genome-wide DNA methylation studies in acute myeloid leukemia. *J Hematol Oncol* 10: 41

40. Figueroa ME, Lugthart S, Li Y, Erpelinck-Verschueren C, Deng X, Christos PJ, Schifano E, Booth J, van Putten W, Skrabanek L, Campagne F, Mazumdar M, Greally JM, Valk PJ, Lowenberg B, Delwel R, Melnick A. 2010. DNA methylation signatures identify biologically distinct subtypes in acute myeloid leukemia. *Cancer Cell* 17: 13-27

41. Qu X, Othus M, Davison J, Wu Y, Yan L, Meshinchi S, Ostronoff F, Estey EH, Radich JP, Erba HP, Appelbaum FR, Fang M. 2017. Prognostic methylation markers for overall survival in cytogenetically normal patients with acute myeloid leukemia treated on SWOG trials. *Cancer* 123: 2472-81

42. Prada-Arismendy J, Arroyave JC, Rothlisberger S. 2017. Molecular biomarkers in acute myeloid leukemia. *Blood Rev* 31: 63-76

43. Ng SW, Mitchell A, Kennedy JA, Chen WC, McLeod J, Ibrahimova N, Arruda A, Popescu A, Gupta V, Schimmer AD, Schuh AC, Yee KW, Bullinger L, Herold T, Gorlich D, Buchner T, Hiddemann W, Berdel WE, Wormann B, Cheok M, Preudhomme C, Dombret H, Metzeler K, Buske C, Lowenberg B, Valk PJ, Zandstra PW, Minden MD, Dick JE, Wang JC. 2016. A 17-gene stemness score for rapid determination of risk in acute leukaemia. *Nature* 540: 433-7

44. Timoty J. Triche SC, Akil Abid Merchant, Preet M Chaudhary, Giridharan Ramsingh. 2014. A DNA methylation signature for stemness in acute myeloid leukemia. *Journal of Clinical Oncology*

45. Huntly BJP. 2013. Role of Epigenetic Readers in Pathogenesis and Therapy of Acute Leukemias. *Blood* 122

46. Huntly B. 2013. The role of BET epigenetic readers in acute myeoid leukemia and other haematological malignancies. *Clinical Epigenetics* 5

47. Mrozek K, Bloomfield CD. 2008. Clinical significance of the most common chromosome translocations in adult acute myeloid leukemia. *J Natl Cancer Inst Monogr*: 52-7

48. Senol Dogan AK-K, Albenita Hajrovic, Muhamed Lisic, Ercan Gokgoz. 2016. Comparison of *MLL* Fusion Genes Expression among the Cytogenetics Abnormalities of Acute Myeloid Leukemia and Their Clinical Effects. *Journal of Biometrics and Biostatistics*

49. Huang S, Yang H, Li Y, Feng C, Gao L, Chen GF, Gao HH, Huang Z, Li YH, Yu L. 2016. Prognostic Significance of Mixed-Lineage Leukemia (*MLL*) Gene Detected by Real-Time Fluorescence Quantitative PCR Assay in Acute Myeloid Leukemia. *Med Sci Monit* 22: 3009-17

50. Winters AC, Bernt KM. 2017. *MLL*-Rearranged Leukemias-An Update on Science and Clinical Approaches. *Front Pediatr* 5: 4

51. Marschalek R. 2016. Systematic Classification of Mixed-Lineage Leukemia Fusion Partners Predicts Additional Cancer Pathways. *Ann Lab Med* 36: 85-100

52. Smith E, Lin C, Shilatifard A. 2011. The super elongation complex (SEC) and *MLL* in development and disease. *Genes Dev* 25: 661-72

53. Biswas D, Milne TA, Basrur V, Kim J, Elenitoba-Johnson KS, Allis CD, Roeder RG. 2011. Function of leukemogenic mixed lineage leukemia 1 (*MLL*) fusion proteins through distinct partner protein complexes. *Proc Natl Acad Sci U S A* 108: 15751-6

54. Cerveira N, Lisboa S, Correia C, Bizarro S, Santos J, Torres L, Vieira J, Barros-Silva JD, Pereira D, Moreira C, Meyer C, Oliva T, Moreira I, Martins A, Viterbo L, Costa V, Marschalek R, Pinto A, Mariz JM, Teixeira MR. 2012. Genetic and clinical characterization of 45 acute leukemia patients with *MLL* gene rearrangements from a single institution. *Mol Oncol* 6: 553-64

55. Liu W, Deng L, Song Y, Redell M. 2014. DOT1L inhibition sensitizes *MLL*-rearranged AML to chemotherapy. *PLoS One* 9: e98270

56. Sykes DB, Kfoury YS, Mercier FE, Wawer MJ, Law JM, Haynes MK, Lewis TA, Schajnovitz A, Jain E, Lee D, Meyer H, Pierce KA, Tolliday NJ, Waller A, Ferrara SJ, Eheim AL, Stoeckigt D, Maxcy KL, Cobert JM, Bachand J, Szekely BA, Mukherjee S, Sklar LA, Kotz JD, Clish CB, Sadreyev RI, Clemons PA, Janzer A, Schreiber SL, Scadden DT. 2016. Inhibition of Dihydroorotate Dehydrogenase Overcomes Differentiation Blockade in Acute Myeloid Leukemia. *Cell* 167: 171-86.e15

57. Kaushik S, Liu F, Veazey KJ, Gao G, Das P, Neves LF, Lin K, Zhong Y, Lu Y, Giuliani V, Bedford MT, Nimer SD, Santos MA. 2018. Genetic deletion or small-molecule inhibition of the arginine methyltransferase PRMT5 exhibit anti-tumoral activity in mouse models of *MLL*-rearranged AML. *Leukemia* 32: 499-509

58. Hatakeyama S. 2017. TRIM Family Proteins: Roles in Autophagy, Immunity, and Carcinogenesis. *Trends Biochem Sci* 42: 297-311

59. Ozato K, Shin DM, Chang TH, Morse HC, 3rd. 2008. TRIM family proteins and their emerging roles in innate immunity. *Nat Rev Immunol* 8: 849-60

60. Belloni E, Trubia M, Gasparini P, Micucci C, Tapinassi C, Confalonieri S, Nuciforo P, Martino B, Lo-Coco F, Pelicci PG, Di Fiore PP. 2005. 8p11 myeloproliferative syndrome with a novel t(7;8) translocation leading to fusion of the FGFR1 and TIF1 genes. *Genes Chromosomes Cancer* 42: 320-5

61. Jain AK, Allton K, Duncan AD, Barton MC. 2014. TRIM24 is a p53-induced E3-ubiquitin ligase that undergoes ATM-mediated phosphorylation and autodegradation during DNA damage. *Mol Cell Biol* 34: 2695-709

62. Allton K, Jain AK, Herz HM, Tsai WW, Jung SY, Qin J, Bergmann A, Johnson RL, Barton MC. 2009. Trim24 targets endogenous p53 for degradation. *Proc Natl Acad Sci U S A* 106: 11612-6

63. Tsai WW, Wang Z, Yiu TT, Akdemir KC, Xia W, Winter S, Tsai CY, Shi X, Schwarzer D, Plunkett W, Aronow B, Gozani O, Fischle W, Hung MC, Patel DJ, Barton MC. 2010. TRIM24 links a non-canonical histone signature to breast cancer. *Nature* 468: 927-32

64. Zhong S, Delva L, Rachez C, Cenciarelli C, Gandini D, Zhang H, Kalantry S, Freedman LP, Pandolfi PP. 1999. A RA-dependent, tumour-growth suppressive transcription complex is the target of the PML-RARalpha and T18 oncoproteins. *Nat Genet* 23: 287-95

65. Le Douarin B, Zechel C, Garnier JM, Lutz Y, Tora L, Pierrat P, Heery D, Gronemeyer H, Chambon P, Losson R. 1995. The N-terminal part of TIF1, a putative mediator of the ligand-dependent activation function (AF-2) of nuclear receptors, is fused to B-raf in the oncogenic protein T18. *Embo j* 14: 2020-33

66. Jain AK, Barton MC. 2009. Regulation of p53: TRIM24 enters the RING. *Cell Cycle* 8: 3668-74

67. Le Douarin B, Nielsen AL, Garnier JM, Ichinose H, Jeanmougin F, Losson R, Chambon P. 1996. A possible involvement of TIF1 alpha and TIF1 beta in the epigenetic control of transcription by nuclear receptors. *Embo j* 15: 6701-15

68. vom Baur E, Zechel C, Heery D, Heine MJ, Garnier JM, Vivat V, Le Douarin B, Gronemeyer H, Chambon P, Losson R. 1996. Differential ligand-dependent interactions between the AF-2 activating domain of nuclear receptors and the putative transcriptional intermediary factors mSUG1 and TIF1. *Embo j* 15: 110-24

69. Torres-Padilla ME, Zernicka-Goetz M. 2006. Role of TIF1alpha as a modulator of embryonic transcription in the mouse zygote. *J Cell Biol* 174: 329-38

70. Lv D, Li Y, Zhang W, Alvarez AA, Song L, Tang J, Gao WQ, Hu B, Cheng SY, Feng H. 2017. TRIM24 is an oncogenic transcriptional co-activator of STAT3 in glioblastoma. 8: 1454

71. Tisserand J, Khetchoumian K, Thibault C, Dembele D, Chambon P, Losson R. 2011. Tripartite motif 24 (Trim24/Tif1alpha) tumor suppressor protein is a novel negative regulator of interferon (IFN)/signal transducers and activators of transcription (STAT) signaling pathway acting through retinoic acid receptor alpha (Raralpha) inhibition. *Nat Commun* 286: 33369-79

72. Lv D, Jia F, Hou Y, Sang Y, Alvarez AA, Zhang W, Gao WQ, Hu B, Cheng SY, Ge J, Li Y, Feng H. 2017. Histone Acetyltransferase KAT6A Upregulates PI3K/AKT Signaling through TRIM24 Binding. *Cancer Res* 77: 6190-201

73. Fang Z, Deng J, Zhang L, Xiang X, Yu F, Chen J, Feng M, Xiong J. 2017. TRIM24 promotes the aggression of gastric cancer via the Wnt/beta-catenin signaling pathway. *Oncol Lett* 13: 1797-806

74. Rafiee MR, Girardot C, Sigismondo G, Krijgsveld J. 2016. Expanding the Circuitry of Pluripotency by Selective Isolation of Chromatin-Associated Proteins. *Mol Cell* 64: 624-35

75. Groner AC, Cato L, de Tribolet-Hardy J, Bernasocchi T, Janouskova H, Melchers D, Houtman R, Cato ACB, Tschopp P, Gu L, Corsinotti A, Zhong Q, Fankhauser C, Fritz C, Poyet C, Wagner U, Guo T, Aebersold R, Garraway LA, Wild PJ, Theurillat JP, Brown M. 2016. TRIM24 Is an Oncogenic Transcriptional Activator in Prostate Cancer. *Cancer Cell* 29: 846-58

76. Appikonda S, Thakkar KN, Barton MC. 2016. Regulation of gene expression in human cancers by TRIM24. *Drug Discov Today Technol* 19: 57-63

77. Miao ZF, Wang ZN, Zhao TT, Xu YY, Wu JH, Liu XY, Xu H, You Y, Xu HM. 2015. TRIM24 is upregulated in human gastric cancer and promotes gastric cancer cell growth and chemoresistance. *Virchows Arch* 466: 525-32

78. Jiang S, Minter LC, Stratton SA, Yang P, Abbas HA, Akdemir ZC, Pant V, Post S, Gagea M, Lee RG, Lozano G, Barton MC. 2015. TRIM24 suppresses development of spontaneous hepatic lipid accumulation and hepatocellular carcinoma in mice. *J Hepatol* 62: 371-9

79. Liu X, Huang Y, Yang D, Li X, Liang J, Lin L, Zhang M, Zhong K, Liang B, Li J. 2014. Overexpression of TRIM24 is associated with the onset and progress of human hepatocellular carcinoma. *PLoS One* 9: e85462

80. Li H, Sun L, Tang Z, Fu L, Xu Y, Li Z, Luo W, Qiu X, Wang E. 2012. Overexpression of TRIM24 correlates with tumor progression in non-small cell lung cancer. *PLoS One* 7: e37657

81. Lin L, Zhao W, Sun B, Wang X, Liu Q. 2017. Overexpression of TRIM24 is correlated with the progression of human cervical cancer. *Am J Transl Res* 9: 620-8

82. Silveira VS, Scrideli CA, Moreno DA, Yunes JA, Queiroz RG, Toledo SC, Lee ML, Petrilli AS, Brandalise SR, Tone LG. 2013. Gene expression pattern contributing to prognostic factors in childhood acute lymphoblastic leukemia. *Leuk Lymphoma* 54: 310-4

83. Quintas-Cardama A, Qiu YH, Post SM, Zhang Y, Creighton CJ, Cortes J, Kornblau SM. 2012. Reverse phase protein array profiling reveals distinct proteomic signatures associated with chronic myeloid leukemia progression and with chronic phase in the CD34-positive compartment. *Cancer* 118: 5283-92

84. Sole F, Espinet B, Sanz GF, Cervera J, Calasanz MJ, Luno E, Prieto F, Granada I, Hernandez JM, Cigudosa JC, Diez JL, Bureo E, Marques ML, Arranz E, Rios R, Martinez Climent JA, Vallespi T, Florensa L, Woessner S. 2000. Incidence, characterization and prognostic significance of chromosomal abnormalities in 640 patients with primary myelodysplastic syndromes. Grupo Cooperativo Espanol de Citogenetica Hematologica. *Br J Haematol* 108: 346-56

85. Cordoba I, Gonzalez-Porras JR, Nomdedeu B, Luno E, de Paz R, Such E, Tormo M, Vallespi T, Collado R, Xicoy B, Andreu R, Munoz JA, Sole F, Cervera J, del Canizo C. 2012. Better prognosis for patients with del(7q) than for patients with monosomy 7 in myelodysplastic syndrome. *Cancer* 118: 127-33

86. Hockendorf U, Yabal M, Herold T, Munkhbaatar E, Rott S, Jilg S, Kauschinger J, Magnani G, Reisinger F, Heuser M, Kreipe H, Sotlar K, Engleitner T, Rad R, Weichert W, Peschel C, Ruland J, Heikenwalder M, Spiekermann K, Slotta-Huspenina J, Gross O, Jost PJ. 2016. RIPK3 Restricts Myeloid Leukemogenesis by Promoting Cell Death and Differentiation of Leukemia Initiating Cells. *Cancer Cell* 30: 75-91

87. Bonnet D, Dick JE. 1997. Human acute myeloid leukemia is organized as a hierarchy that originates from a primitive hematopoietic cell. *Nat Med* 3: 730-7

88. Pollyea DA, Gutman JA, Gore L, Smith CA, Jordan CT. 2014. Targeting acute myeloid leukemia stem cells: a review and principles for the development of clinical trials. *Haematologica* 99: 1277-84

89. Collins CT, Hess JL. 2016. Deregulation of the HOXA9/MEIS1 axis in acute leukemia. *Curr Opin Hematol* 23: 354-61

90. Gentles AJ, Plevritis SK, Majeti R, Alizadeh AA. 2010. Association of a leukemic stem cell gene expression signature with clinical outcomes in acute myeloid leukemia. *Jama* 304: 2706-15

91. Boulais PE, Frenette PS. 2015. Making sense of hematopoietic stem cell niches. *Blood* 125: 2621-9

92. Blank U, Karlsson S. 2015. TGF-beta signaling in the control of hematopoietic stem cells. *Blood* 125: 3542-50

93. Zhang CC, Lodish HF. 2008. Cytokines regulating hematopoietic stem cell function. *Curr Opin Hematol* 15: 307-11

94. Riether C, Schürch CM, Ochsenbein AF. 2015. Regulation of hematopoietic and leukemic stem cells by the immune system. *Cell Death Differ* 22: 187-98

95. Zhang CC. 2012. Hematopoietic stem cells: interplay with immunity. *Am J Blood Res* 2: 219-27

96. Schepers K, Campbell TB, Passegué E. 2015. Normal and Leukemic Stem Cell Niches: Insights and Therapeutic Opportunities. *Cell Stem Cell* 16: 254-67

97. Lane SW, Scadden DT, Gilliland DG. 2009. The leukemic stem cell niche: current concepts and therapeutic opportunities. *Blood* 114: 1150-7

98. Perez-Lloret J, Okoye IS, Guidi R, Kannan Y, Coomes SM, Czieso S, Mengus G, Davidson I, Wilson MS. 2016. T-cell-intrinsic Tif1alpha/Trim24 regulates IL-1R expression on TH2 cells and TH2 cell-mediated airway allergy. *Proc Natl Acad Sci U S A* 113: E568-76

99. Gechijian LN, Buckley DL, Lawlor MA, Reyes JM, Paulk J, Ott CJ, Winter GE, Erb MA, Scott TG, Xu M, Seo HS, Dhe-Paganon S, Kwiatkowski NP, Perry JA, Qi J, Gray NS.

2018. Functional TRIM24 degrader via conjugation of ineffectual bromodomain and VHL ligands.

Vita:

Justin Parker Shaw was born in Pine Bluff Arkansas, the son of Richard and Charla Shaw. After completing his degree at Houston High School, Germantown, Tennessee, in 2010, he was admitted to the University of Tennessee. After two years, he transferred to Texas A&M. While there, he worked as an undergraduate research assistant in the Department of Microbial Pathogenesis & Immunology under the guidance of Dr. Julian Leibowitz, as well as simultaneously a separate undergraduate research assistant position in the Department of Biology under Dr. Ginger Carney. After publishing as first-author the results of a project with the Center for Phage Technology, led by Dr. Ryland Young, Justin graduated from Texas A&M with a B.S. in genetics in May of 2015. The following fall, he entered The University of Texas MD Anderson Cancer Center UTHealth Graduate School of Biomedial Sciences, and has since been under the mentorship and guidance of Dr. Margarida Santos.

Permanent address:

7550 Kirby Drive
Apartment 732
Houston, Texas 77030